

Grotesque: Complex Geometric Arrangement of Unreflected HEU (93.15) Metal Pieces

Mackenzie L. Gorham
John D. Bess

September 2011



The INL is a U.S. Department of Energy National Laboratory
operated by Battelle Energy Alliance

Grotesque: Complex Geometric Arrangement of Unreflected HEU (93.15) Metal Pieces

**Mackenzie L. Gorham
John D. Bess**

September 2011

**Idaho National Laboratory
Idaho Falls, Idaho 83415**

<http://www.inl.gov>

**Prepared for the
U.S. Department of Energy
Office of National Nuclear Security Administration
Under DOE Idaho Operations Office
Contract DE-AC07-05ID14517**

**GROTESQUE: COMPLEX GEOMETRIC ARRANGEMENT
OF UNREFLECTED HEU (93.15) METAL PIECES**

Evaluators

Mackenzie L. Gorham
Idaho State University/ U.S. Department of Energy - Idaho

John D. Bess
Idaho National Laboratory

Internal Reviewers

John D. Bess
J. Blair Briggs
Idaho National Laboratory

Richard L. Dickson
U.S. Department of Energy - Idaho

Independent Reviewers

John T. Mihalcz
Oak Ridge National Laboratory

Daniel F. Hollenbach
Spectra Tech Inc.

GROTESQUE: COMPLEX GEOMETRIC ARRANGEMENT OF UNREFLECTED HEU (93.15) METAL PEICES

IDENTIFICATION NUMBER: HEU-MET-FAST-081

SPECTRA

KEYWORDS: acceptable, bare, complex geometry, critical experiment, GROTESQUE, highly-enriched, unmoderated, unreflected, uranium

1.0 DETAILED DESCRIPTION

1.1 Overview of Experiment

The GROTESQUE experiments were designed specifically to develop and test neutronics for the GEOM subroutine of the 05R code.^a Two complex arrangements of various highly enriched uranium metal cylinders, rectangular parallelepipeds, and spheres were arranged in a circular formation on a steel diaphragm. A centerpiece was raised remotely through a hole in the steel diaphragm to achieve criticality.

The first arrangement consisted of five major units, each major unit consisting of a stack of smaller uranium pieces. The second arrangement utilized nine major units, again consisting of stacks of smaller uranium pieces. The 9-unit arrangement is the only experiment discussed in this evaluation, since the five stack experiment never achieved criticality. The 9-unit arrangement is shown in Figure 1.1.

The experiments were performed at the Oak Ridge Critical Experiments Facility (ORCEF) in June 1964. The 9-unit configuration was later used as part of the development process for early versions of KENO and a model representing a variation of this experiment (Sample Problem 7: GROTESQUE without the Diaphragm) is released with modern versions of SCALE for testing the proper installation of the KENO module.^b

An experimental report for the GROTESQUE experiment has not been published; however there are two publications that describe the experiment (References 1 and 2). A separate report^c discussing the conversion of the 05r model into a KENO model was published; however, the author did not consult with the experimenter for GROTESQUE. This report is considered unreliable (except for dimensions) by the experimenter and should not be used to obtain information pertinent to the GROTESQUE experiment.^d The Oak Ridge Critical Experiments Facility (ORCEF) Logbook 15r contains the primary documentation from the experimenter for this experiment.^e

The lower support structures were used in several other experiments, including those evaluated in [HEU-MET-FAST-069](#) and [HEU-MET-FAST-059](#). The upper support structure consisting of a thick aluminum plate is shown in Figure 8 of [HEU-MET-FAST-076](#). The HEU metal cylinders were used

^a D.C. Irving, et al. "05R, A General Purpose Monte Carlo Neutron Transport Code," ORNL-3622, Oak Ridge National Laboratory (1965). Dave Irving coined the name (GROTESQUE) for this assembly when he first saw the photograph.

^b S. Goluoglu, D. F. Hollenbach, and L. M. Petrie, "CSAS6: Control Module for Enhanced Criticality Safety Analysis with KENO-VI," ORNL/TM-2005/39 ver. 6, vol. I, sect. C6, Oak Ridge National Laboratory (2009).

^c J. R. Knight, "GROTESQUE Without Tears," ORNL/CSD/TM-220, Oak Ridge National Laboratory (1984).

^d Personal communication with John T. Mihalcz, April 2011.

^e Oak Ridge Critical Experiments Facility Logbook 15r, "Book 4," pp. 30-50.

previously in the Tinkertoy experiments,^a [HEU-MET-FAST-023](#), [HEU-MET-FAST-026](#), and [HEU-MET-FAST-054](#). The GROTESQUE arrangement of nine major units was evaluated and determined to be an acceptable benchmark experiment.

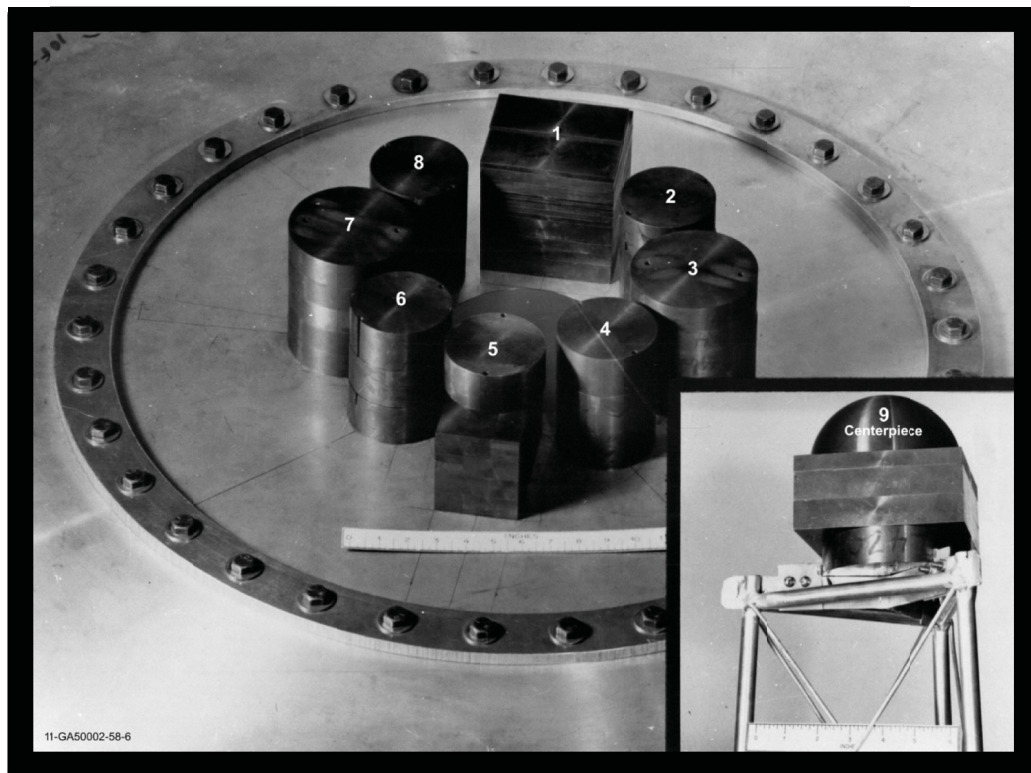


Figure 1.1. Photograph of GROTESQUE Experimental Assembly (inset not to scale).
(Aluminum support plate is visible outside the clamping ring.)

1.2 Description of Experimental Configuration

1.2.1 HEU Units – This experiment uses nine numbered HEU units comprised of many smaller component pieces of HEU stacked together. The major units consist of six cylinder combinations; one irregular combination of three rectangular parallelepipeds (rpp); one hemisphere on top of a rectangular parallelepiped with a cylinder beneath it; and one cylinder and parallelepiped combination. There are two 0.508 cm diameter holes drilled through the cylinders at a spacing of 8.547 cm apart (as shown in Figures 1.2 through 1.10). All cylinders were located so that their holes were along a diameter through the center of the system. The 5-in. metal slabs used to assemble Units 1, 5, and 9 were reported to have been used in a previous experiment^b as well (Reference 3).^c The experimenter that performed the experiments in [HEU-MET-FAST-056](#) reported the densities of the cylinders as slightly lower than they actually are, because the small holes were calculated as having been homogenized into the units.

^a Personal communication between J. Blair Briggs and John Mihalcz, July 2010.

^b J. T. Mihalcz and J. J. Lynn, "Critical Parameters of Bare and Reflected 93.4 wt.% U235-Enriched Uranium Metal Slabs," ORNL-3016, Oak Ridge National Laboratory (December 1960), p. 73-76.

^c ORCEF Logbooks 119R and 116R.

HEU-MET-FAST-081

Table 1.1 contains the dimensions for each of the nine major units; in the cases of more complex geometries, Table 1.1 refers to the largest outer dimensions. The dimensions of the smaller component pieces were recorded in the experimental logbook,^a and are shown in Tables 1.2 through 1.10. The order in which the smaller component pieces were stacked to create the larger major units is not specified, except for the centerpiece, which is clearly labeled in the logbook.^b

Table 1.1. Nominal Dimensions of the Major HEU Units in cm.^(a,b)

Unit Number	Description	X Dimension	Y Dimension	Z Dimension (height)	Diameter
1	Irregular RPP ^(c)	12.703	12.703	13.377 ^(d)	-
2	Cylinder	-	-	12.918	9.111
3	Cylinder	-	-	13.475	11.522
4	Cylinder	-	-	12.969	9.105
5	Complex RPP	12.703	7.620	13.229 ^(d)	9.146 ^(e)
6	Cylinder	-	-	12.974	9.109
7	Cylinder	-	-	13.475	11.499
8	Cylinder	-	-	12.954	9.113
9	Centerpiece ^(f)	-	-	-	-

(a) ORCEF Logbook 15r, p. 44.

(b) J. R. Knight, "GROTESQUE Without Tears," ORNL/CSD/TM-220, Oak Ridge National Laboratory (1984).

(c) Rectangular Parallelepiped.

(d) Dimension for highest point of stack.

(e) The radius applied to the cylinder stacked on the RPP; refer to Figure 1.6 for clarification.

(f) The centerpiece is a complex combination of several units, and is described in Figure 1.10.

Figures 1.2 through 1.10 are detailed depictions of the major units. Please note that although in Figures 1.2 through 1.10 the units appear solid, many were actually stacks of smaller component pieces (see Figure 1.1).

Tables 1.2 through 1.10 summarize the dimensions of the component pieces that comprise each unit. Only nominal dimensions in inches, which were rounded, are provided for each individual piece. The overall dimensions in Figures 1.2 through 1.10 for each unit are more precisely known and are reported in centimeters.^c Nominal part dimensions and masses were obtained from the experimental logbook.^d Nominal dimensions for slabs were reported in Reference 3 as well; however, the manufacturing tolerances were reported as ± 0.002 in. The actual dimensional tolerances at Y-12 machining during this time period were certainly less than 0.002 in.^e

^a ORCEF Logbook 15r, pp. 30-49.

^b ORCEF Logbook 15r, p. 44.

^c J. R. Knight, "GROTESQUE Without Tears," ORNL/CSD/TM-220, Oak Ridge National Laboratory (1984).

^d ORCEF Logbook 15r, pp. 44-45.

^e Personal communication with John T. Mihalcz, August 2011.

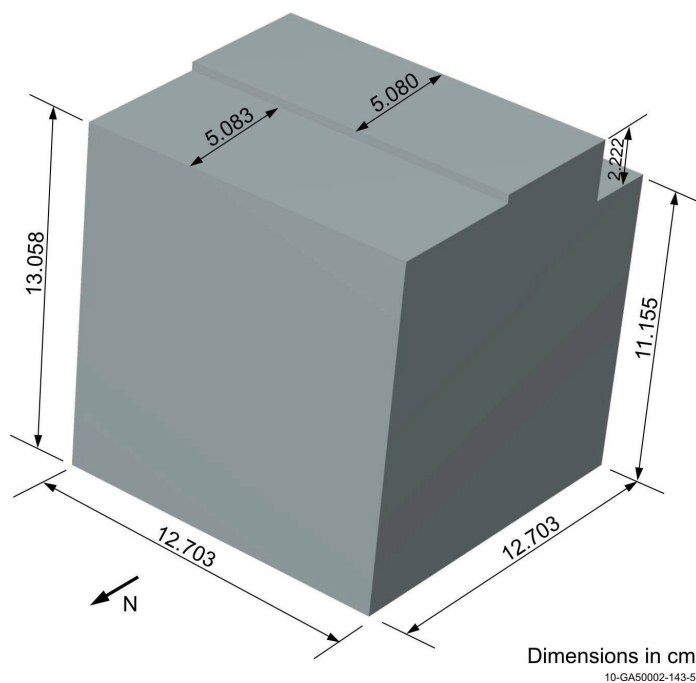
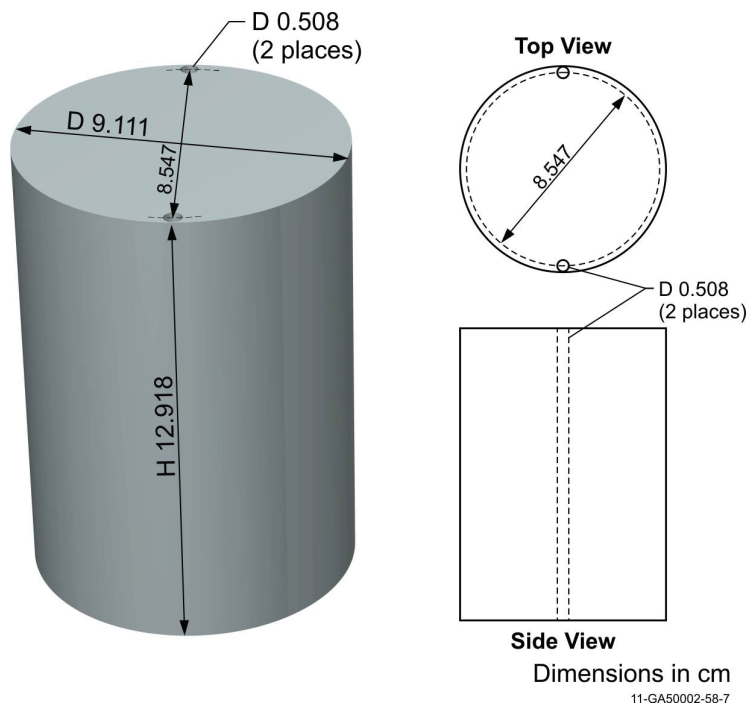


Figure 1.2. Unit 1.

Table 1.2. Nominal Dimensions of Unit 1 Component Pieces.

Part Number	Type	Length (in.)	Width (in.)	Height (in.) ^(a)	Mass (g)
1011	rpp	5	5	7/8	6689
0971	rpp	5	5	1/2	3827
0970	rpp	3	5	1/2	3822
1010	rpp	5	5	7/8	6695
0950	rpp	3	5	1/4	1916
0955	rpp	3	5	1/4	1916
1023	rpp	2	5	1/8	963
1024	rpp	2	5	1/8	963
1048	rpp	2	5	1/8	961
0957	rpp	3	5	1/4	1918
1916	rpp	3	5	1/2	3846
0974	rpp	3	5	1/5	1534
0975	rpp	3	5	1/5	1533
0948	rpp	2	5	1/10	765
0960	rpp	2	5	1/10	768
0995	rpp	1	5	1/10	381

(a) Nominal heights (Personal communication with John T. Mihalcz, August 2011).



11-GA50002-58-7

Figure 1.3. Unit 2.

Table 1.3. Nominal Dimensions of Unit 2 Component Pieces.

Part Number	Type	Height (in.)	Diameter (in.)	Mass (g)
2284	Cylinder	1.7	3.57	5195
2285	Cylinder	1.7	3.57	5287
2286	Cylinder	1.7	3.57	5286

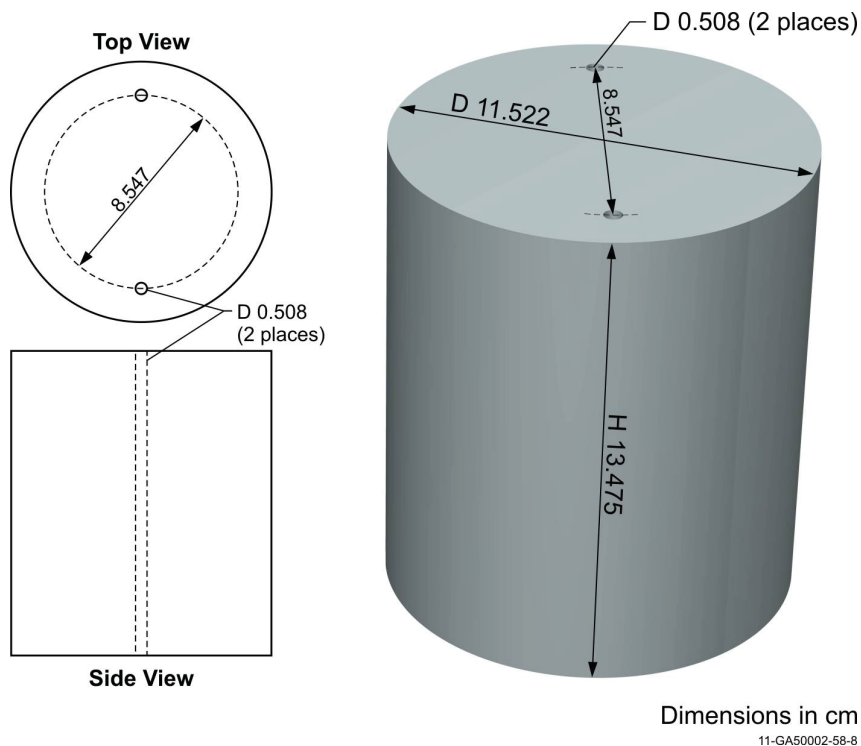


Figure 1.4. Unit 3.

Table 1.4. Nominal Dimensions of Unit 3 Component Pieces.

Part Number	Type	Height (in.)	Diameter (in.)	Mass (g)
2460	Cylinder	1.06	4.53	5250
2462	Cylinder	1.06	4.53	5237
2463	Cylinder	1.06	4.53	5258
2464	Cylinder	1.06	4.53	5219
2466	Cylinder	1.06	4.53	5252

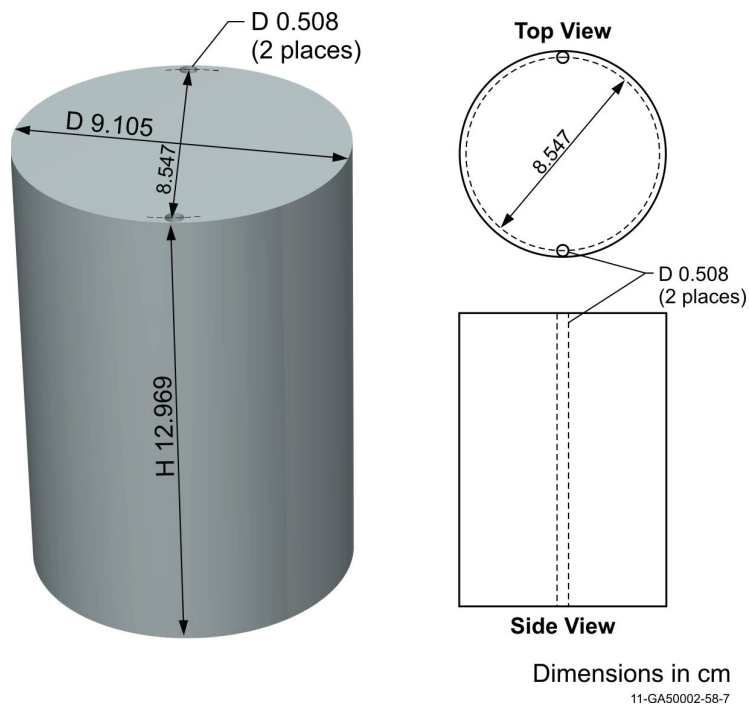


Figure 1.5. Unit 4.

Table 1.5. Nominal Dimensions of Unit 4 Component Pieces.

Part Number	Type	Height (in.)	Diameter (in.)	Mass (g)
2278	Cylinder	1.7	3.57	5267
2279	Cylinder	1.7	3.57	5219
2280	Cylinder	1.7	3.57	5234

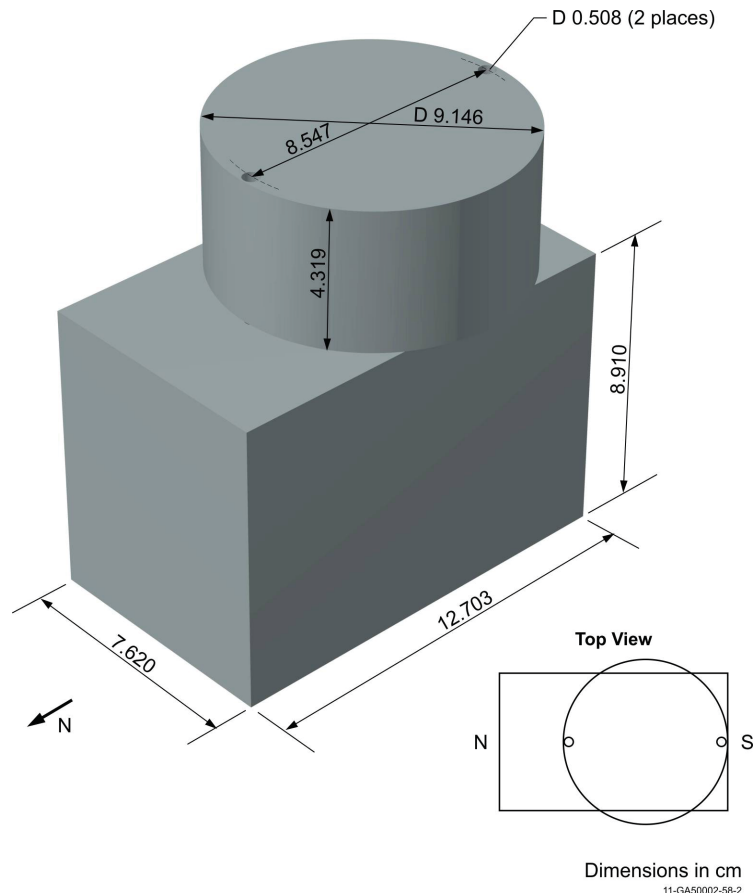


Figure 1.6. Unit 5.
(The cylinder was aligned along the center of the block
with its edge flush with the end of the block.)

Table 1.6. Nominal Dimensions of Unit 5 Component Pieces.

Part Number	Type	Length (in.)	Width (in.)	Height (in.) ^(a)	Diameter (in.)	Mass (g)
945	rpp	5	2	-	-	2679
943	rpp	5	2	-	-	2680
944	rpp	5	2	-	-	2682
946	rpp	5	2	-	-	2682
1085	rpp	5	1	-	-	1346
942	rpp	5	1	-	-	1341 ^(b)
979	rpp	5	1	-	-	769
962	rpp	5	1	-	-	383
1032	rpp	5	1	-	-	192
978	rpp	5	1	-	-	768
963	rpp	5	1	-	-	383
1014	rpp	5	1	-	-	193
2572	cylinder	-	-	1.7	3.57	5286

(a) Height measurements were not provided for each piece. Slab piece heights could be 7/8, 1/2, 1/4, or 1/8 in. (Reference 3).

(b) Page 36 of the experimental logbook lists this value as 1161 g whereas Page 45 lists the value as 1341 g. The correct value was 1341 g.

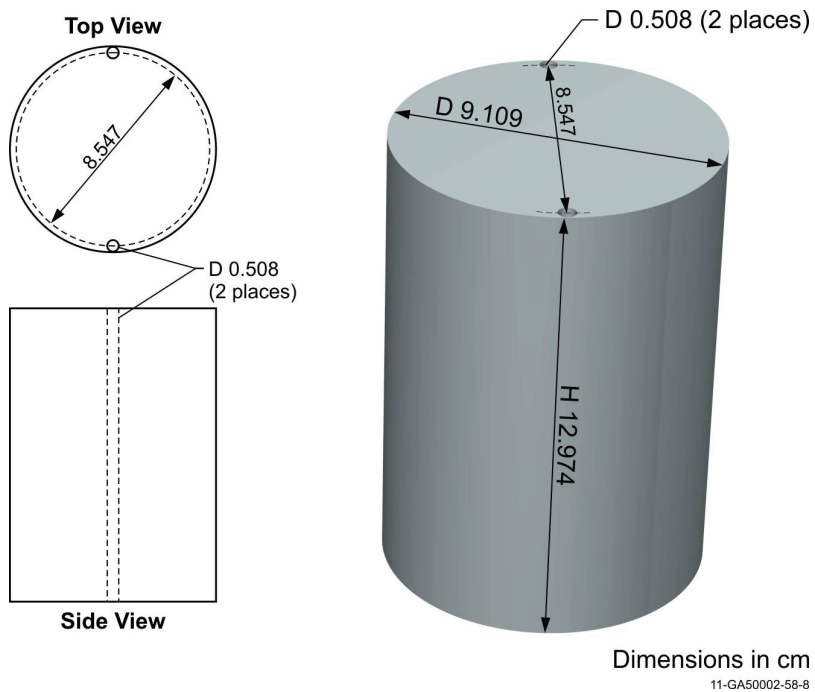


Figure 1.7. Unit 6.

Table 1.7. Dimensions of Unit 6 Component Pieces.

Part Number	Type	Height (in.)	Diameter (in.)	Mass (g)
2281	cylinder	1.7	3.57	5259
2282	cylinder	1.7	3.57	5220
2283	cylinder	1.7	3.57	5248

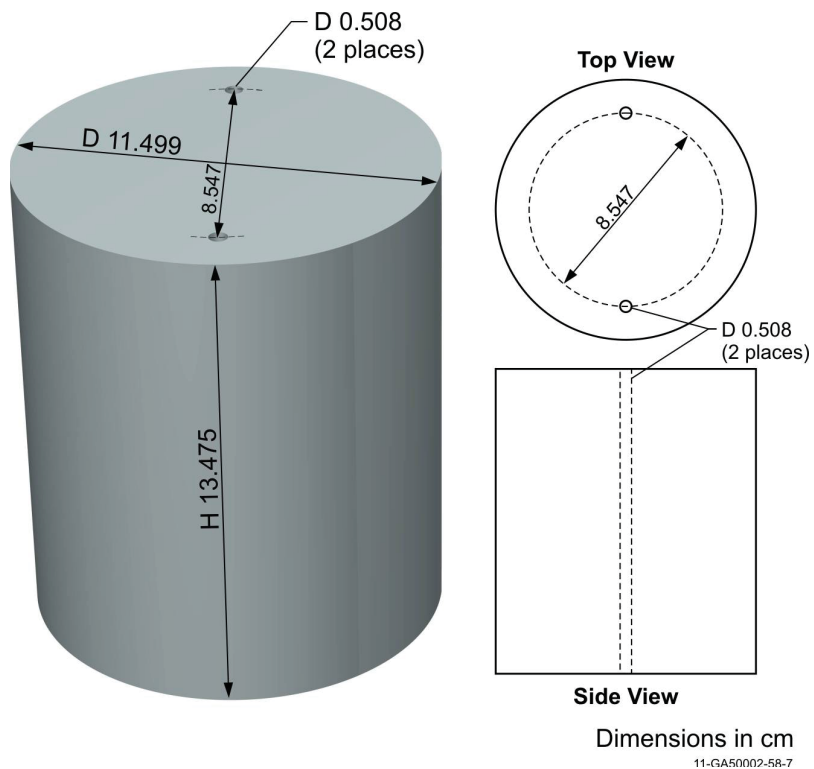


Figure 1.8. Unit 7.

Table 1.8. Nominal Dimensions of Unit 7 Component Pieces.

Part Number	Type	Height (in.)	Diameter (in.)	Mass (g)
2467	cylinder	1.06	4.53	5251
2468	cylinder	1.06	4.53	5224
2469	cylinder	1.06	4.53	5217
2471	cylinder	1.06	4.53	5226
2472	cylinder	1.06	4.53	5242

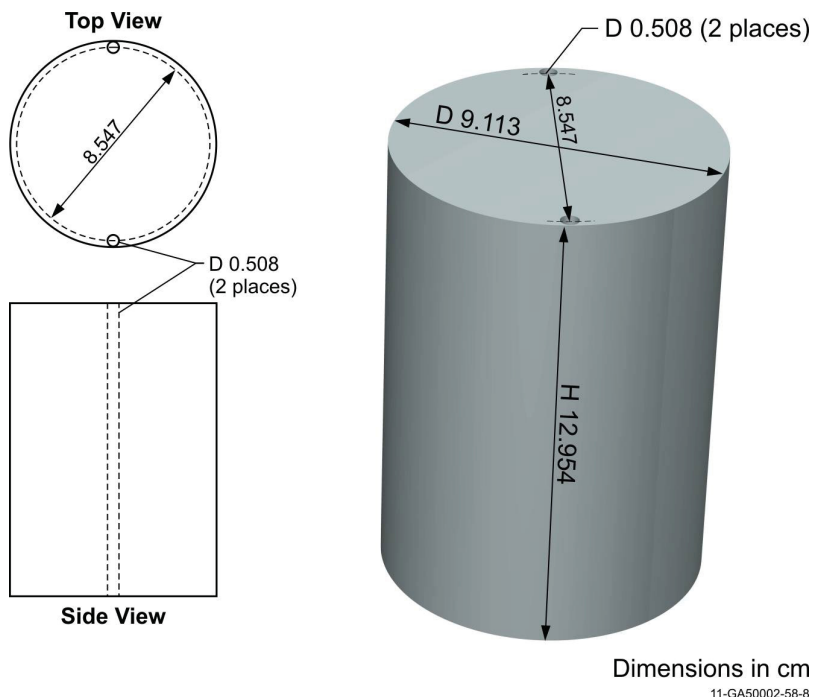


Figure 1.9. Unit 8.

Table 1.9. Nominal Dimensions of Unit 8 Component Pieces.

Part Number	Type	Height (in.)	Diameter (in.)	Mass (g)
2571	cylinder	1.7	3.57	5231
2276	cylinder	1.7	3.57	5254
2277	cylinder	1.7	3.57	5270

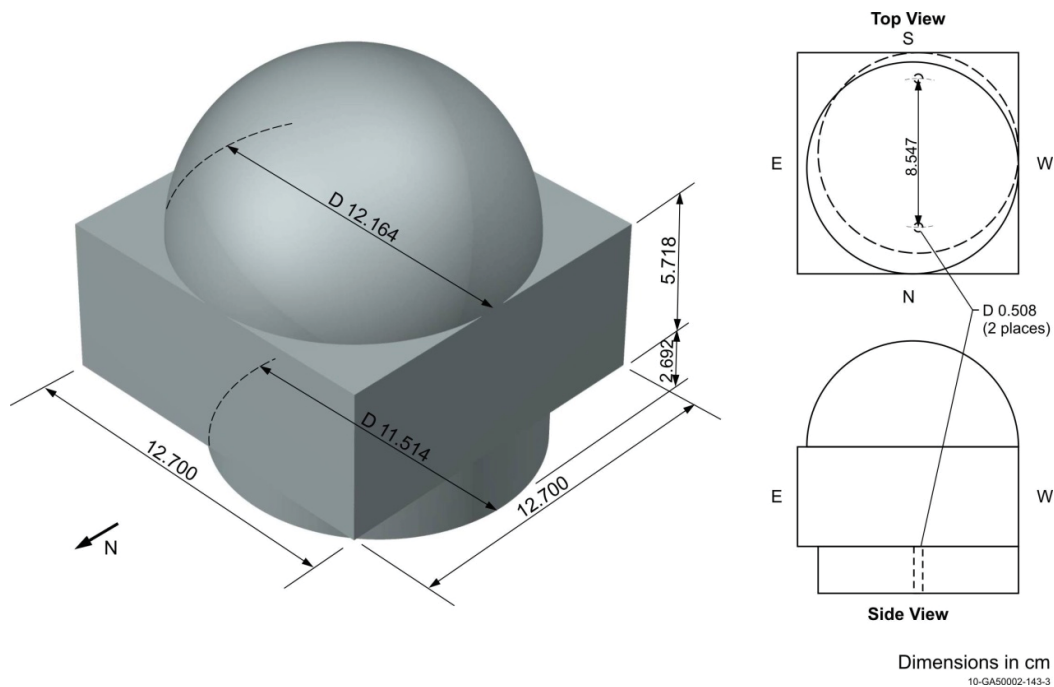


Figure 1.10. Unit 9 (Centerpiece).

Table 1.10. Nominal Dimensions of Unit 9 Component Pieces.

Part Number	Type	Length (in.)	Width (in.)	Height (in.)	Diameter (in.)	Mass (g)
2470	cylinder	-	-	1.06	4.53	5247
1008	rpp	5	5	7/8	-	6693
1012	rpp	5	5	7/8	-	6684
967	rpp	5	5	1/2	-	3833
3380	hemisphere	-	-	-	4.8	8838

The experimenter rounded in some cases when reporting the summed total mass for each unit in the logbook. The most accurate total mass is calculated by adding the mass reported in the logbook for each of the individual component pieces without rounding, which is the procedure used in this report.

HEU-MET-FAST-081

It should be noted that the large mass of the HEU units caused the steel diaphragm that supported them to sag when all the units were placed on the assembly. This caused the pieces to be slightly tilted towards the center of the assembly. The tilt angle for each major unit is described in Table 1.11.^a

Tilt angles were measured using a dial gauge accurate to one-thousandth of an inch to determine the deflection of the units due to the diaphragm sag. The placement of the units was also measured. Reported uncertainty in the measurement of the deflection of the steel diaphragm is 0.005 in. (0.0127 cm) and the uncertainty in the placement of the HEU units is 0.010 in. (0.0254 cm).^b The distance from the hole in the diaphragm to the bottom face of Units 1 through 8 were 0.750, 0.624, 0.579, 0.365, 0.755, 0.380, 0.588, and 0.591 in., respectively.^c

Table 1.11. Measured Tilt Angle for HEU Units.^(a)

Unit	1	2	3	4	5	6	7	8	9
Tilt Angle (°)	1.350	1.400	1.173	1.970	2.580	1.680	1.400	1.100	0.0

(a) Knight, J.R., "GROTESQUE Without Tears," ORNL/CSD/TM-220, Oak Ridge National Laboratory (1984).
The values were calculated using the measurements reported in the previous paragraph and unit dimensions.

1.2.2 Steel Diaphragm – The stainless steel diaphragm is 10 mil thick (0.0254 cm) and secured by a clamping ring apparatus bolted to a 0.50-in.-thick aluminum plate (see Figure 1.12) that has a 30 in. (76.2 cm) inside diameter.^d There is a 7.25 in. (18.415 cm) diameter hole cut in the center of the diaphragm through which the centerpiece is passed via remote operation.^b The diaphragm support assembly was used in other ORCEF benchmark experiments, including [HEU-MET-FAST-076](#). The Vertical Assembly Machine used to support the aluminum plate is shown in Figure 1.11.

1.2.3 Other Supports – Certain components from this experiment were used in other benchmark experiments ([HEU-MET-FAST-059](#) and [HEU-MET-FAST-069](#)). The detailed drawings of the lower support stand that held the centerpiece is provided as Figure 17 in [HEU-MET-FAST-059](#). The apparatus used in this experiment (see Figure 1.11) was a "vertical assembly machine, which primarily consisted of a hydraulic lift (22-inch vertical motion) to support the lower section and a stationary upper section." A typical support structure for bare HEU experiments performed at the ORCEF is shown in Figure 1.12. A low mass lower support stand like the one mounted on the vertical lift in Figure 1.12 was also mounted on the vertical lift for this measurement. The upper support apparatus shown in Figure 1.11 held an aluminum plate with a 30-in.-diameter hole. The interior of this plate was machined to accept the clamping ring which, when attached (bolted), held the stainless steel (304L) diaphragm in place and in tension.^e The plate was shaped to hold the diaphragm in tension when the bolts were tightened in a prescribed manner.^f

^a Personal communication with John T. Mihalcz, May 2010; use angle values reported in J. R. Knight, "GROTESQUE Without Tears," ORNL/CSD/TM-220, Oak Ridge National Laboratory (1984).

^b Personal communication with John T. Mihalcz, August 2010.

^c ORCEF Logbook 15r, p 44.

^d ORCEF Logbook 15r, p. 35.

^e Personal communication with John T. Mihalcz, April 2011.

^f Personal communication with John T. Mihalcz, August 2011.

The entire support structure consisted of at least a support plate, a support ring, and a support stand, in addition to the diaphragm discussed in Section 1.2.2. There are measurements recorded in the logbook that were performed to determine the worth of the different support structures.^a The diaphragm was measured individually to be worth 10.19 ϵ of reactivity^b and the entire support structure was valued at 10.2 ϵ of reactivity. An additional measurement using two 10-mil diaphragms was also reported. The second diaphragm was attached under the first one; since it was so light compared to what was on the diaphragm already, it did not change the deflection. This configuration was used to measure the worth of the diaphragms as 19.29 ϵ . Those measurements clearly show that the diaphragm is the primary contributor to the worth of the support structures.

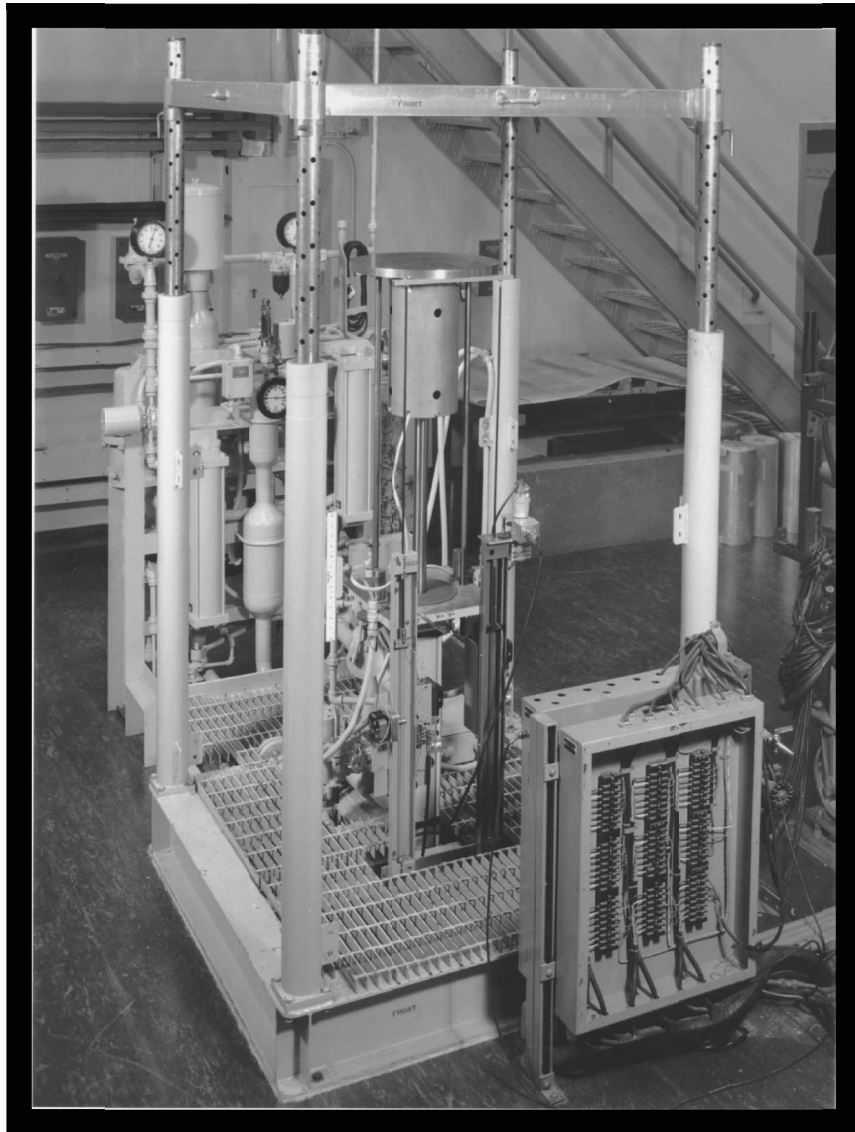


Figure 1.11. Photograph of the Vertical Assembly Machine.
(The upper support shown was used to hold the 0.5-in.-thick aluminum plate that supported the upper section for this experiment and a low mass support stand was mounted on the vertical lift.)

^a ORCEF Logbook 15r, p. 49.

^b ORCEF Logbook 15r, p. 48.

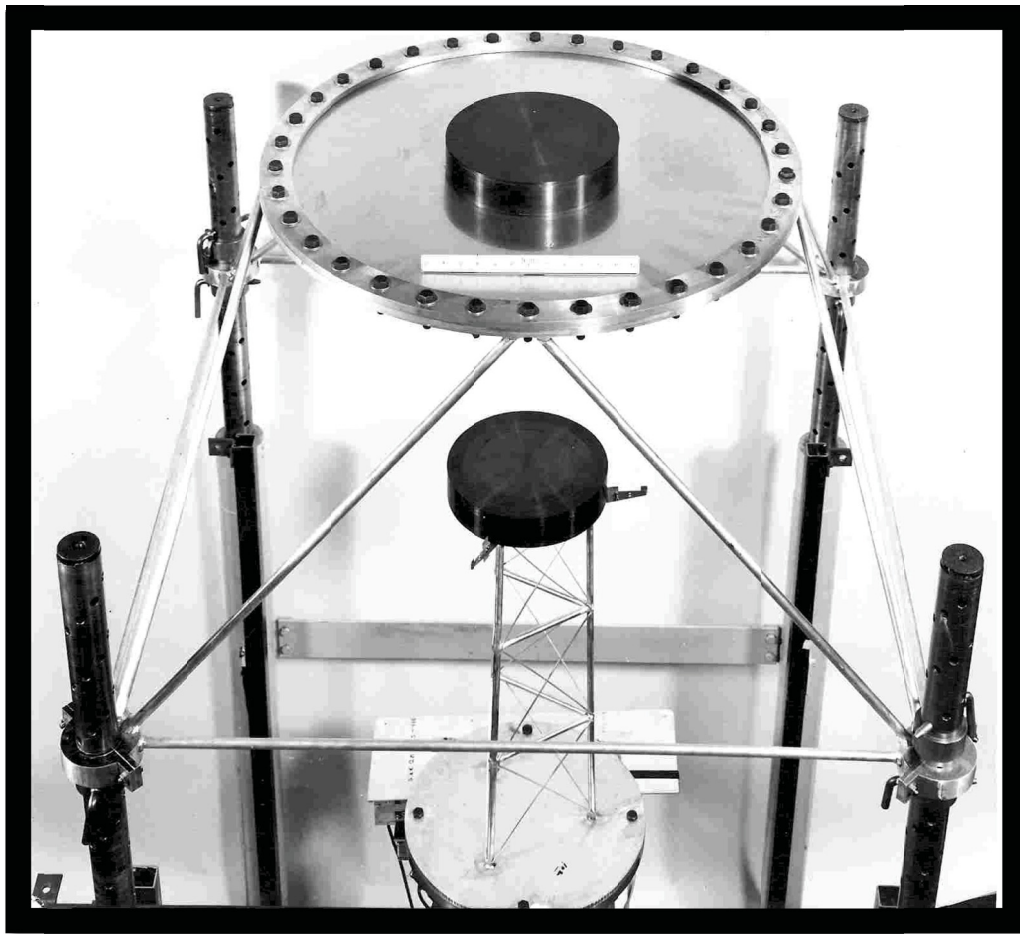


Figure 1.12. A Typical Uranium Metal Assembly of Two Interacting 11-inch-Diameter Cylinders at Close Spacing on the Vertical Assembly Machine.^a
(The experiment shown is an example of the typical support structure used and does not represent the actual GROTESQUE experiment except for the lower support stand, vertical lift, and four support poles.)

1.2.4 Assembly Description – The pieces were arranged in a circular manner on a thin steel diaphragm with a hole through its center, as shown in Figure 1.1. The inset on the figure shows the centerpiece, and is not to scale; however, it is comparable in size to the other major units.

The centerpiece rises through the hole that is slightly visible in the center of the major units in Figure 1.1. Raising the centerpiece from the bottom side of the diaphragm into the ring of HEU units to increase the system k_{eff} was done remotely.

Figure 1.13 shows the top view of the experimental configuration, as well as the numbering scheme for the major units. The north-pointing arrow aligns with the y-axis and dimensions presented in tables reflect this. The upper dimension refers to the distance of the base of the units from the corresponding axis. The lower dimension reported indicate the distance to the midplane of the unit. Figure 1.13 was created using the information from Table 1.12 to determine the coordinates of each unit and its placement

^a Photo 39380, Oak Ridge National Laboratory photo of a bare uranium assembly.

within the circle of units. This information is from the primary reference and detailed sketches in the logbook.

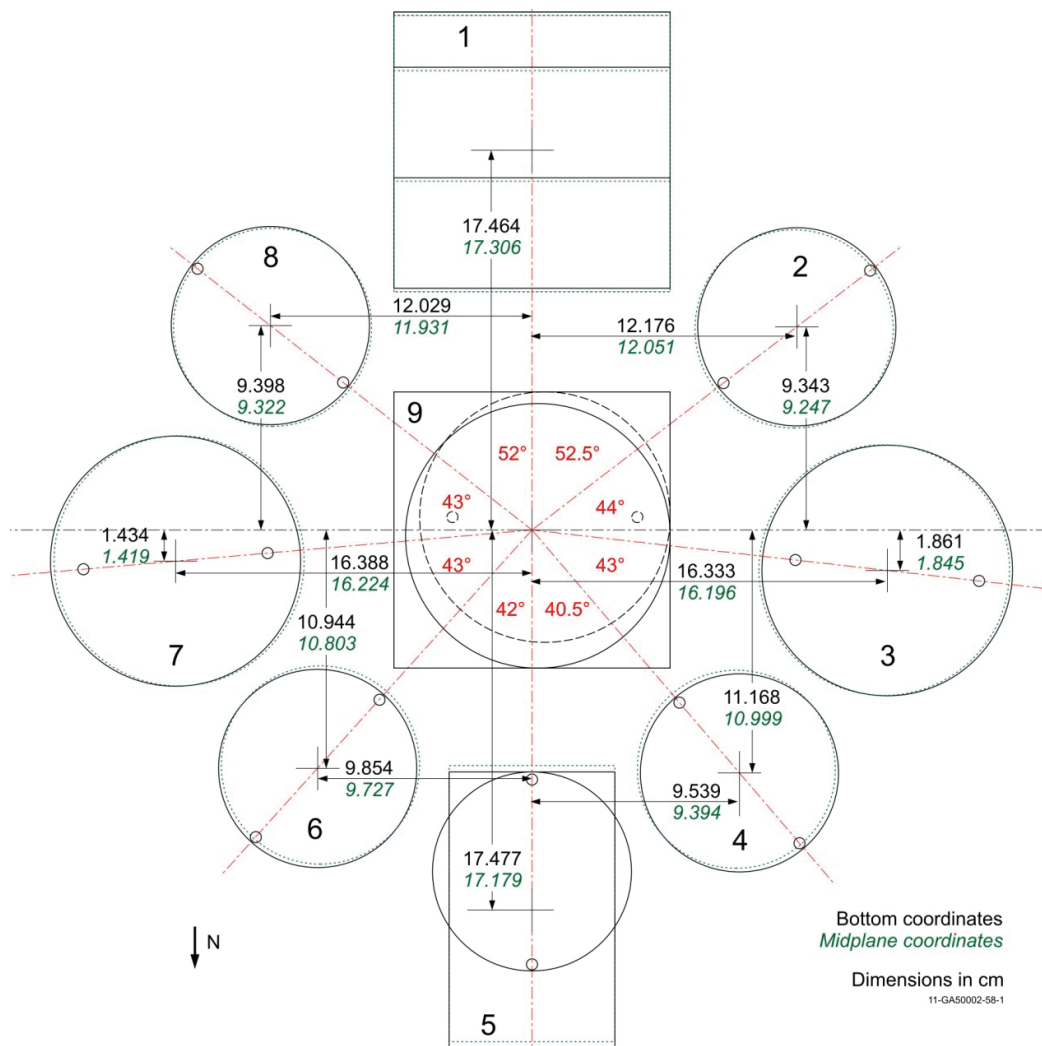


Figure 1.13. Placement of GROTESQUE Experimental Assembly Units (top view).

Table 1.12. Assembly Geometry Positioning.^(a)

Unit Number	Distance from Hole (cm) ^(e)	Angular Spacing (°)	Center Bottom X Coordinate (cm)	Center Bottom Y Coordinate (cm)	Center Bottom Z Coordinate (cm)
1	1.905	270.0	0.0	-17.464	0.150
2	1.585	217.5	-12.176	-9.343	0.111
3	1.471	173.5	-16.333	1.861	0.174
4	0.927	130.5	-9.539	11.168	0.156
5 ^(b)	1.918	90.0	0.0	17.477	0.290
5 ^(c)	3.464	90.0	0.0	15.698 ^(c)	9.2
6	0.965	48.0	9.854	10.944 ^(f)	0.134
7	1.494	5.0	16.388	1.434	0.140
8	1.501	322.0	12.029	-9.398	0.087
9 ^(c)	0.0	-	-0.593	-0.593	-1.755
9 ^(b)	0.0	-	0.0	0.0	0.937
9 ^(d)	0.0	-	-0.268	0.268	6.655

(a) Knight, J.R., "GROTESQUE Without Tears," ORNL/CSD/TM-220, Oak Ridge National Laboratory (1984). The x,y coordinates were derived from the hole distance, angular spacing, and unit dimensions.

(b) Rectangular parallelepiped component piece.

(c) Cylinder component piece.

(d) Hemisphere component piece.

(e) The distance from the hole in the diaphragm to the bottom faces of the peripheral units. These values had been calculated from the original measurements in inches by converting to centimeters; the number of decimal places had been truncated.

(f) This value was incorrectly reported as 10.964. The correct value, which corresponds to the angular spacing and distance from the hole reported in this table, is provided here.

1.2.5 k_{eff} Data – The experimental k_{eff} value was reported in the experimental logbook^a and was determined through stable reactor period measurements. The reactivity was obtained from the reactor period using the Inhour equation. The logbook also provides information on a repeatability measurement. The inferred k_{eff} value of the primary experiment and the value inferred for the repeatability measurements are presented below in Table 1.13. There were several additional k_{eff} values published for this experiment; however, they were from models created in various codes (References 1 and 2) and not direct measurements.^{b,c} Uncertainties were not provided for individual measurements. However, the uncertainty in the measurement of k_{eff} is evaluated in Section 2.6.

^a ORCEF Logbook 15r, pp. 47-48.

^b J. T. Mihalczo, "Prompt-Neutron Lifetime in Critical Enriched-Uranium Metal Cylinders and Annuli," *Nucl. Sci. Eng.*, **20**, 60-65 (1965).

^c J. T. Mihalczo, "Critical Experiments and Calculations with Annular Cylinders of U(93.2) Metal," ORNL-3499, Oak Ridge National Laboratory (1963).

HEU-MET-FAST-081

Table 1.13. Measured Reactivity Data.^(a)

Experiment	Date	Measured Reactivity (€)
Experiment 4 ^(b)	6-15-64	-9.20 and -9.05
Experiment 1 ^(c)	6-16-64	-7.87 and -8.47

(a) There were additional reactivity measurements recorded on pp. 49-50 of the logbook, but they do not represent repeatability measurements. They were measurements for different configurations with varying heights of the centerpiece (Personal Communication with John T. Mihalczco, March 2011).

(b) ORCEF Logbook 15r, p. 47.

(c) ORCEF Logbook 15r, p. 48, repeat of Experiment 4 from p. 47.

1.3 Description of Material Data

1.3.1 HEU Metal Pieces – The uranium pieces were all reported to be enriched to 93.15 wt.%,^{a,b} Often enrichments of 93.15 wt.% were sometimes rounded to 93.2 wt.% when reported. Two different uranium mixtures are actually present in the GROTESQUE experiment. The HEU cylinders were used in the Tinkertoy experiments and have been evaluated in [HEU-MET-FAST-023](#) and [HEU-MET-FAST-026](#).^a In addition, the metal slabs stacked to create the rectangular pieces of the units were also used in previous experiments (Reference 3). The slab pieces were earlier incorrectly reported elsewhere as enriched to 93.4 wt.% ²³⁵U,^c but were also enriched to 93.15 wt.%.^d The uranium metal enrichments are listed in Table 1.14.

Table 1.14. GROTESQUE Isotopic Composition (References 1 and 3).

Isotope	Cylinder Content (wt.%) ^(a)	Slab Content (wt.%)
²³⁴ U	0.97	1.07
²³⁵ U	93.15	93.15
²³⁶ U	0.24	0.68
²³⁸ U	5.64	5.10

(a) These values are rounded in Reference 1 and are reported in the Tinkertoy experiments: [HEU-MET-FAST-023](#) and [HEU-MET-FAST-026](#).

The isotopic composition of the hemisphere in Unit 9 is not recorded but is very close to those in other oralloy measurements in the East cell of ORCEF.^e

The total masses of each unit are given in Table 1.15, and the densities calculated from the masses and dimensions (Figure 1.2 through 1.10) are also provided.

^a J. T. Mihalczco, "Prompt-Neutron Lifetime in Critical Enriched-Uranium Metal Cylinders and Annuli," *Nucl. Sci. Eng.*, **20**, 60-65 (1965).

^b Personal communication between John T. Mihalczco and J. Blair Briggs, July 2010.

^c J. T. Mihalczco and J. J. Lynn, "Critical Parameters of Bare and Reflected 93.4 wt.% U235-Enriched Uranium Metal Slabs," ORNL-3016, Oak Ridge National Laboratory (December 1960), p. 73-76.

^d Personal communication with John T. Mihalczco, June 2011.

^e Personal communication with John T. Mihalczco, August 2011.

HEU-MET-FAST-081

Table 1.15. Total Mass and Density of the HEU Units.

Unit Number	Total Mass (g)	Unit Density (g/cm ³) ^(d)
1	38497	18.63085
2	15768	18.83944 ^(e)
3	26216	18.73198
4	15720	18.73305
5	21384 ^(a)	18.68481
6	15727	18.71762
7	26160	18.76711
8	15755	18.76331
9	31295 ^(b)	18.70980
Total	206522 ^(c)	18.71875 ^(f)

- (a) The mass of the rectangular parts sum to 16098 g, but the summation of these parts is reported as 16100 g in the logbook. The mass of the entire stack, including the cylindrical component, sums to 21384 g even though the logbook reports 21386 g.
- (b) The logbook rounds to 31300 g when the summation of the individual pieces is 31295 g.
- (c) The total mass loading is reported as 216.529 kg in the logbook, which is slightly larger than the summation of the individual parts.
- (d) Mass density of the units was calculated by the evaluator. The number of significant figures retained in the mass density does not represent the precision of the measurements but enables duplication of atom densities in the benchmark specifications.
- (e) This mass density is higher than typical HEU material; however, it was computed directly from available mass and volume data.
- (f) The standard density of oralloy at this time from Y-12 data sheets was 18.75 g/cm³; personal communication with John T. Mihalczo, April 2011.

Impurity data for the uranium units were not available. Typical impurity data for HEU metal used at ORCEF during this time period are shown in Table 2.11.

1.3.2 Steel Diaphragm – The stainless steel diaphragm was Type 304L.^a

1.3.3 Support Structure – An aluminum clamping ring with stainless steel bolts was used to hold the stainless steel diaphragm. A description of these materials is not relevant since the reactivity effect was measured and the experimental configuration reactivity was corrected for their removal.^b

1.4 Temperature Data

No mention of the system temperature was made in the report or logbook. According to the experimenter, the ORCEF operated at a nominal temperature of 293 K.^c The fission rate in the measurements usually corresponded to much less than 0.01 watts, so there was no appreciable heating of the experimental components. Typically the dimensions of the uranium component pieces used in ORCEF experiments were measured at 70 °F and the experiments were performed at 72 °F. The reactivity coefficient for temperature for these assemblies is approximately -0.3 ρ /°C.^d

^a Personal communication with John T. Mihalczo, April 2011.

^b Personal communication with John T. Mihalczo, January 2011.

^c Personal communication with John T. Mihalczo, February 2010.

^d Personal communication with John T. Mihalczo, March 2010 and August 2010.

1.5 Supplemental Experimental Measurements

Rossi alpha measurements at delayed criticality were performed but were never formally documented and the results do not appear in the logbook.^a

^a Personal communication with John T. Mihalczo, August 2011.

2.0 EVALUATION OF THE EXPERIMENTAL DATA

Monte Carlo N-Particle (MCNP) version 5-1.51^a calculations were utilized to estimate the biases and uncertainties associated with the experimental results in this evaluation. MCNP is a general-purpose, continuous-energy, generalized-geometry, time-dependent, coupled n-particle Monte Carlo transport code. The Evaluated Neutron Data File library, ENDF/B-VII.0,^b was utilized in this evaluation. The 1 σ statistical uncertainty associated with the MCNP calculations was ± 0.00002 for all calculations. The uncertainty in Δk is 0.00003. Calculations were performed with 1,000,000 neutrons per cycle for 1,000 active cycles after skipping 50 cycles; the total number of neutron histories was 1,000,000,000. For this report, an uncertainty is considered negligible if Δk is ≤ 0.00010 .

The detailed benchmark model provided in Section 3 was utilized with perturbations of the model parameters to estimate uncertainties in k_{eff} due to uncertainties in parameter values defining the experimental configuration. Where applicable, comparison of the upper and lower perturbation k_{eff} values to evaluate the uncertainty in the eigenvalue were utilized to minimize correlation effects, if any, induced by comparing all perturbations to the original benchmark model configuration, as discussed elsewhere.^c

Unless specifically stated otherwise, all uncertainty values in this section correspond to 1 σ . When the change in k_{eff} between the base case and the perturbed model, or two perturbed models, was less than the statistical uncertainty of the Monte Carlo results, the changes in the variable were amplified, if possible, and the calculations repeated. The resulting calculated change was then scaled back corresponding to the actual uncertainty, assuming linearity.

The total evaluated uncertainty for this experiment is provided in Section 2.7. The square root of the sum of the squares of all the individual uncertainties assessed in this section is used to obtain the total uncertainty in the experimental k_{eff} . As discussed in Section 2.1.1, all uncertainties are treated as 100% systematic, with no reduction due to randomness in the uncertainty values.

The GROTESQUE experiment has been evaluated and judged to be an acceptable benchmark experiment.

2.1 β_{eff}

There were no recorded β_{eff} measurements for this experiment. Other similar experiments^d provide a β_{eff} of 0.0067, which is typical for the uranium enrichment used. The experimenter recommends using the value of 0.0067.^e It is typical to assume a 5% uncertainty in β_{eff} , according to related benchmarks [HEU-MET-FAST-059](#) and [HEU-MET-FAST-069](#). Therefore, the calculated β_{eff} for this experiment is 0.0067 ± 0.00034 .

^a X-5 Monte Carlo Team, "MCNP – a General Monte Carlo n-Particle Transport Code, version 5," LA-UR-03-1987, Los Alamos National Laboratory (2003).

^b M. B. Chadwick, et al., "ENDF/B-VII.0: Next Generation Evaluated Nuclear Data Library for Nuclear Science and Technology," *Nucl. Data Sheets*, **107**: 2931-3060 (2006).

^c D. Mennerdahl, "Statistical Noise for Nuclear Criticality Safety Specialists," *Trans. Am. Nucl. Soc.*, **101**: 465-466 (2009).

^d J. T. Mihalczo, "Critical Experiments and Calculations with Annular Cylinders of U(93.2) Metal," ORNL-3499, Oak Ridge National Laboratory (1963).

^e Personal communication with John T. Mihalczo, August 2011.

2.2 HEU Pieces

2.2.1 Unit Worths – The worth of each of the nine units was calculated by comparing the benchmark model in Section 3 with models in which each individual unit was removed. The worth was converted into reactivity, ρ \$, and plotted against unit mass (see Table 2.1 and Figure 2.1). As expected, the worth of the centerpiece (Unit 9) is the greatest. The worth of the other eight units does increase with increasing mass; however, there is no direct correlation between unit mass and worth. Because of the variation in unit worth for this configuration, all uncertainties are treated as 100% systematic with no correction for randomness in measurement.

Table 2.1. Calculated Worth of Each Unit.

Unit	Worth (ρ \$)	Mass (kg)
1	-5.32	38.5
2	-2.66	15.8
3	-3.34	23.2
4	-2.41	15.7
5	-2.05	21.4
6	-2.22	15.7
7	-3.12	23.2
8	-2.56	15.8
9	-11.89	31.3

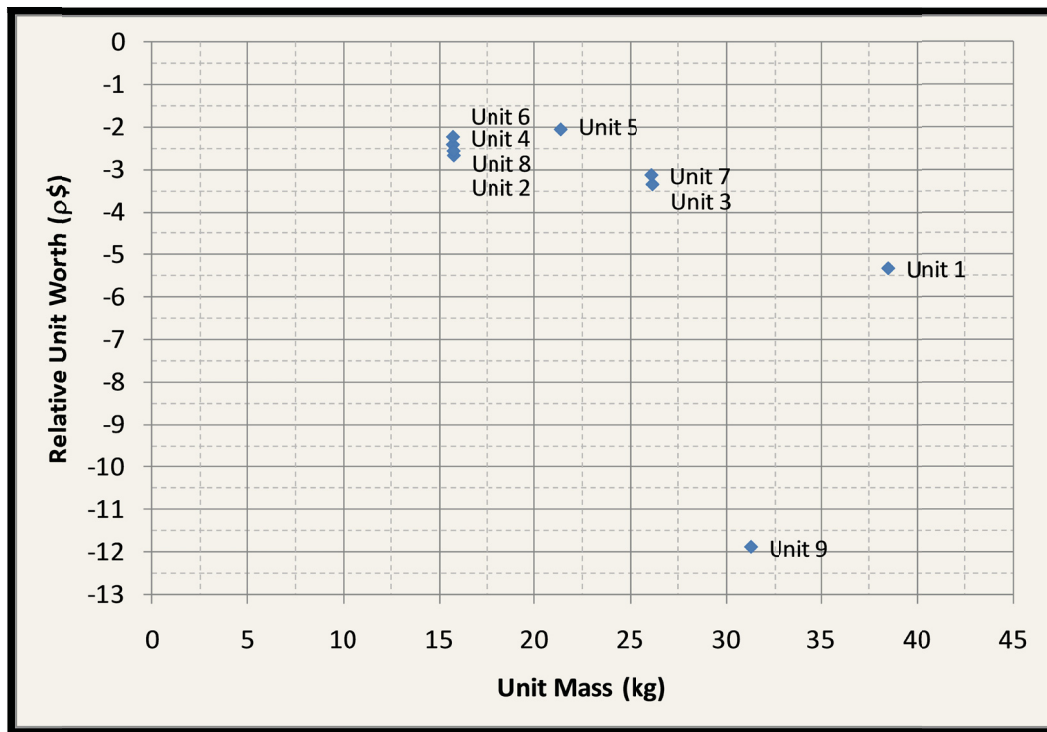


Figure 2.1. Relative Unit Worth.

2.2.2 Homogenization of Units – The nine major units are made up of individual pieces stacked together. There would have been small gaps between each piece that could allow for some streaming. Detailed dimensions of each individual part were not available. Units were considered homogenous for this evaluation, with the densities calculated in Section 2.2.4. The uncertainty in the homogenization of the GROTESQUE units is considered to be negligible since the effect for removing the gaps and overall dimensional uncertainty were determined to be negligible (Section 3.1.1.1 and Section 2.2.6). For units with multiple types of pieces (e.g., cylinders and slabs) the homogenization was assumed for each sub-unit region, single cylinder or rectangular parallelepiped, respectively.

The effect of homogenizing the holes in the cylindrical pieces into the unit was demonstrated to be small compared to the total simplification bias for the simple benchmark model (Section 3.1.2). Therefore, the uncertainty in the diameter, location, or orientation of the holes was also judged to be negligible.

2.2.3 Gaps between Pieces – No information was provided on gap size, so a reasonable approximation of twice the machining tolerance of ± 0.002 in. (± 0.00508 cm) was used to estimate the effect of gaps between individual pieces of each unit. Actual gap thicknesses would be comparable to those found in [HEU-MET-FAST-051](#), which are considerably smaller in size than the tolerance value used in this evaluation.^a No uncertainty was evaluated for the size of these gaps because removing them created a negligible bias, as discussed in Section 3.1.1.1. Therefore, the total macroscopic dimensions and mass are preserved for this analysis, and gaps and their associated uncertainties are ignored.

2.2.4 Density – The density of each unit was calculated using the reported masses and unit dimensions (see Figure 1.2 through 1.10 and Table 1.15). A summary of unit volumes, masses, and densities is reproduced in Table 2.2. The density of each unit was calculated using the reported masses and unit volumes (see Figures 1.2 through 1.10). A summary of unit volumes, masses, and densities is reproduced in Table 2.1. Units 5 and 9 are comprised of different geometry types. These subunit parts are separated into single table entries.

The small support holes were ignored in the simple model and homogenized into the units, giving a slightly higher unit volume and lower density. Using the given mass and calculated volumes, the homogenized density of each unit was calculated (Table 2.3).

An average mass density was determined (both with and without holes) by dividing the total mass of all units by the total volume (both with and without holes) of all units used in the GROTESQUE experiment. The average density of the HEU units with holes included in the cylindrical pieces is 18.72 g/cm^3 ; it is 18.66 g/cm^3 when the holes are neglected (i.e., homogenized into the units).

^a Personal communication with John T. Mihalczko, August 2011.

HEU-MET-FAST-081

Table 2.2. Evaluated Density Data (including holes).

Unit	Mass (g)	Volume (cm ³)	Density (g/cm ³) ^(a)
1	38497	2066.3039	18.63085
2	15768	836.9674	18.83944
3	26216	1399.5315	18.73198
4	15720	839.1585	18.73305
5-slabs	16098	862.4600	18.66521
5-cylinder	5286	281.9990	18.74475
6	15727	840.2244	18.71762
7	26160	1393.9278	18.76711
8	15755	839.6707	18.76331
9-cylinder	5247	279.2051	18.79264
9-slabs	17210	922.2562	18.66076
9-hemisphere	8838	471.1919	18.75669

(a) The number of significant figures retained in the mass density does not represent the precision of the measurements but enables duplication of atom densities in the benchmark specifications.

Table 2.3. Evaluated Density Data (without holes).

Unit	Mass (g)	Volume (cm ³)	Density (g/cm ³) ^(a)
1	38497	2066.3039	18.63085
2	15768	842.2039	18.72231
3	26216	1404.9938	18.65916
4	15720	844.4156	18.61642
5-slabs	16098	862.4600	18.66521
5-cylinder	5286	283.7497	18.62909
6	15727	845.4836	18.60119
7	26160	1399.3901	18.69386
8	15755	844.9218	18.64670
9-cylinder	5247	280.2963	18.71948
9-slabs	17210	922.2562	18.66076
9-hemisphere	8838	471.1919	18.75669

(a) The number of significant figures retained in the mass density does not represent the precision of the measurements but enables duplication of atom densities in the benchmark specifications.

2.2.5 HEU Mass – Mass measurements for each component piece, as well as the major units, are provided in the logbook.^a The total masses of each unit are shown in Table 1.15.

The measurements are reported to the nearest gram, but no description of the measurement technique or accuracy is provided in the primary reference. Evaluations of several other experiments (HEU-MET-FAST-051, HEU-MET-FAST-059, HEU-MET-FAST-069, HEU-MET-FAST-071, and HEU-MET-FAST-076) performed at the same facility by the same experimenter with HEU material used a value of uncertainty in the mass of each HEU part of ± 0.5 g. The mass uncertainty is based on calibration standards from the Bureau of Standards that were used to calibrate the scales for measuring uranium masses at the Y-12 Plant, which were accurate to less than 0.5 g for parts weighing up to 20 kg.^b

^a ORCEF Logbook 15r, p. 45.

^b Personal communication with John T. Mihalczko, April 2011.

HEU-MET-FAST-081

These previous experiments indicate that the measurements were also rounded to the nearest gram, which is consistent with the reporting format in the experimental logbook.

To find the effect of this uncertainty on the k_{eff} value, the mass of each HEU piece from Tables 1.2 – 1.10 were adjusted by a factor of 3 times the 1σ uncertainty of 0.5 g. In order to keep the total uranium volume of the experiment constant, the density of each of the uranium unit was adjusted accordingly. The combined total 1σ uncertainty in mass was 28 g, which is much greater than an estimated uncertainty of ~5 g (0.5 g / 20 kg \times 206.5 kg). Any additional mass uncertainty due to wearing of parts, oxidation, hydrating, and oil are negligible. The calculated uncertainty in k_{eff} due to the uncertainty in HEU mass is shown in Table 2.4.

Table 2.4. HEU Mass Uncertainty.

Deviation	Δk	\pm	$\sigma_{\Delta k}$	Scaling Factor	$\Delta k_{\text{eff}} (1\sigma)$	\pm	$\sigma_{\Delta k_{\text{eff}}}$
± 84 g	0.00029	\pm	0.00001	3	0.00010	\pm	<0.00001

2.2.6 HEU Dimensions – The major uranium units were comprised of smaller component pieces that were used in other experiments at the ORCEF. No information was provided in the logbook regarding machining tolerances or measurement precision; however, these uranium pieces from the same facility that were used by the same experimenter in other projects near the same time period were described as being dimensionally accurate (i.e., having a manufacturing tolerance) to within 0.002 in. (0.00508 cm).^a Reference 3 also states that the machining tolerances for the HEU slabs were 0.002 in. (0.00508 cm). Calculations were performed in which the dimensions of all HEU pieces were increased by 0.00508 cm and then subsequently decreased by 0.00508 cm. Figures 1.1 through 1.10 and Tables 1.2 through 1.10 were used to approximate the number of pieces stacked in the experiment or placed side-by-side. A summary of the evaluated number of pieces in each dimension for each unit is provided in Table 2.5. Mass was conserved by adjusting the density of the units. The heights, diameters, lengths, widths, and thicknesses of every piece was simultaneously increased or decreased by the manufacturing tolerance assuming all uncertainties were 100% systematic. The uncertainty in k_{eff} due to the uncertainty in the HEU dimensions was still determined to be negligible (see Table 2.6).

Actual gap thicknesses would be comparable to those found in [HEU-MET-FAST-051](#), which are considerably smaller in size than the tolerance value used in this evaluation.^b Even when using the manufacturing tolerance of ± 0.002 in. provided above, which is much larger than the actual dimensional uncertainty, the calculated uncertainty in k_{eff} is still negligible.

^a J. T. Mihalcz, “Prompt-Neutron Lifetime in Critical Enriched-Uranium Metal Cylinders and Annuli,” *Nucl. Sci. Eng.*, **20**, 60-65 (1965).

^b Personal communication with John T. Mihalcz, August 2011.

HEU-MET-FAST-081

Table 2.5. Number of Pieces across Each Unit.

Unit	Dimension	# Pieces	Type	Unit	Dimension	# Pieces	Type
1	Height	~12	Slabs	6	Height	3	Cylinders
	Width	1	Slabs		Diameter	1	Cylinders
	Length	~2	Slabs			3	Total
		16	Total	7	Height	5	Cylinders
2	Height	3	Cylinders		Diameter	1	Cylinders
	Diameter	1	Cylinders			5	Total
		3	Total	8	Height	3	Cylinders
3	Height	5	Cylinders		Diameter	1	Cylinders
	Diameter	1	Cylinders			3	Total
		5	Total	9	Height	1	Cylinder
4	Height	3	Cylinders		Height	3	Slabs
	Diameter	1	Cylinders		Height	1	Hemisphere
		3	Total		Width	1	Slabs
5	Height	~6	Slabs		Length	1	Slabs
	Height	1	Cylinder		Diameter	1	Cylinder
	Width	<3	Slabs		Diameter	1	Hemisphere
	Length	1	Slabs			5	Total
	Diameter	1	Cylinder				
		13	Total				

Table 2.6. HEU Dimensional Uncertainty.

Deviation	Δk	\pm	$\sigma_{\Delta k}$	Scaling Factor	$\Delta k_{\text{eff}} (1\sigma)$	\pm	$\sigma_{\Delta k_{\text{eff}}}$
0.00508 cm per piece per dimension	-0.00001	\pm	0.00001	1	-0.00001	\pm	0.00001

2.2.7 HEU Tilt Angle – The tilt angles can be calculated using trigonometric ratios of the distance from the center of the experiment, distance to the midpoint of each periphery unit, and the deflection of the given unit. The deflection ratio is the ratio of the vertical deflection over the radius (or distance) from the deflected position to a given point (in this case, the front face of the periphery unit). The arctangent of the deflection ratio provides the tilt angle. Thus a perturbation in either the measured distance from the center of the experiment or the vertical deflection would impact the calculated tilt angle. Uncertainty in the dimensions of the HEU units would have a negligible impact on the total uncertainty in the tilt angle.

The measurements for the tilt angle and coordinates of the HEU units were reported to 3 significant digits, which may not reflect the accuracy to which these measurements were performed. The uncertainty in the measured deflection of the diaphragm is 0.005 in. (0.0127 cm) and the uncertainty in the measure of the bottom center coordinates of the fissile material is 0.010 in. (0.0254 cm).^a This method maximizes the uncertainty in the angle.

The uncertainty in the tilt angle of the HEU units was determined by adjusting the unit positions by ± 0.010 in. (0.0254 cm) from the center of the diaphragm and simultaneously moving the parts ± 0.005 inches (0.0127 cm) up or down in deflection. These changes were used to calculate the uncertainty in the

^a Personal communication with John Mihalcz, April 2011.

HEU-MET-FAST-081

tilt angle for each unit. The changes in the angle due to the uncertainty in axial deflection and radial placement are shown in Table 2.7.

Table 2.7. HEU Tilt Angle Uncertainty.

Unit	Center Bottom X,Y Coordinates (cm)	Bottom Z Coordinate (cm)	Center Middle X,Y Coordinates (cm)	Deflection Ratio	Reported Angle (°)	Angle Uncertainty (°)
1	0.000, -17.464	0.150	0.000, -17.306	0.0236	1.350	0.066
2	-12.176, -9.343	0.111	-12.051, -9.247	0.0244	1.400	0.068
3	-16.333, 1.861	0.174	-16.196, 1.845	0.0205	1.173	0.068
4	-9.539, 11.168	0.156	-9.394, 10.999	0.0344	1.970	0.072
5	0.0, 15.698	0.290	0.000, 15.400	0.0451	2.580	0.066
6	9.854, 10.944	0.134	9.727, 10.803	0.0293	1.680	0.072
7	16.388, 1.434	0.140	16.224, 1.419	0.0244	1.400	0.068
8	12.029, -9.398	0.087	11.931, -9.322	0.0192	1.100	0.068
--	--	--	--	--	average	0.068

The change in k_{eff} due to the uncertainty in the deflection of the HEU units was calculated by using the average of the calculated changes in the angles from Table 2.7. To determine the effects of uncertainty, the tilt angle was increased and decreased by 0.068° . This is a 1σ uncertainty and is not corrected by the number of perturbed units because correlation effects between the units would not be equal due to the difference in their individual worth (see Section 2.2.1.) The effective uncertainty in k_{eff} due to the uncertainty in the tilt angle is reported in Table 2.8. Because the maximum tilt angle was calculated by perturbing the 1σ uncertainties in the deflection and radial position, the calculated uncertainty in k_{eff} is divided by $\sqrt{2}$.

Table 2.8. HEU Tilt Uncertainty.

Deviation	Δk	\pm	$\sigma_{\Delta k}$	Scaling Factor	$\Delta k_{\text{eff}} (1\sigma)$	\pm	$\sigma_{\Delta k_{\text{eff}}}$
$\pm 0.068^\circ$	0.00024	\pm	0.00001	$\sqrt{2}$	0.00017	\pm	0.00001

2.2.8 HEU Isotopic Content – The isotopic data for the GROTESQUE experiment is provided in Table 1.14; these values are reproduced in Table 2.9 for comparison with the mass-weighted average isotopic composition (assuming all HEU material had the same isotopic content). The isotopic values for the cylinders were initially assumed to best represent those for the hemisphere used in the central unit.^a However, an average of the isotopic compositions could also be used. The effective bias and uncertainty in selecting the isotopic composition of the hemisphere is negligible compared to the overall benchmark experiment uncertainty.

^a Personal communication with John T. Mihalczko, April 2011.

HEU-MET-FAST-081

Table 2.9. Uranium Isotopic Content.

Isotope	Cylinder and Hemisphere Content (wt.%)	Slab Content (wt.%)	Mass-Weighted Average Content (wt.%)
^{234}U	0.97	1.07	1.00
^{235}U	93.15	93.15	93.15
^{236}U	0.24	0.68	0.39
^{238}U	5.64	5.10	5.46

Based on these data, and similar treatment of isotopic uncertainties for HEU parts used in [HEU-MET-FAST-059](#) and [HEU-MET-FAST-069](#), a reasonable estimate of the uncertainty in the average isotopic measurements for the cylinders is ± 0.005 wt.%. Each isotope's weight percent was adjusted by ± 0.15 wt.% (thirty times the 1σ uncertainty of ± 0.005 wt.%), and the ^{238}U content was adjusted to maintain a total isotopic sum of 100%. The uncertainty in the isotopic composition of the slabs and cylinders were perturbed simultaneously since there was not a significant difference in their contents. The effect of the total uranium isotopic uncertainty is presented in Table 2.10.

The uncertainty in the isotopic composition of the hemisphere is greater than the perturbations evaluated as the exact composition was unknown. It is known that the HEU metal used in the hemisphere would be very close in composition to the cylinder and slab compositions. Perturbation of the hemisphere isotopic compositions within the range of values provided in Table 2.9 provides negligible additional uncertainty to the benchmark experiment.

Table 2.10. Uranium Isotopic Uncertainty.

Deviation	Δk	\pm	$\sigma_{\Delta k}$	Scaling Factor	$\Delta k_{\text{eff}} (1\sigma)$	\pm	$\sigma_{\Delta k_{\text{eff}}}$
± 0.15 wt.% ^{234}U	0.00053	\pm	0.00001	30	0.00002	\pm	<0.00001
± 0.15 wt.% ^{235}U	0.00076	\pm	0.00001	30	0.00003	\pm	<0.00001
± 0.15 wt.% ^{236}U	0.00017	\pm	0.00001	30	0.00001	\pm	<0.00001

2.2.9 HEU Impurities – No impurity data were provided for the HEU units used in the GROTESQUE experiment. However, these parts were produced at the same time as those for which isotopic data was available. Data from [HEU-MET-FAST-059](#), [HEU-MET-FAST-069](#), [HEU-MET-FAST-071](#), and [HEU-MET-FAST-076](#) were used as a good approximation of the effect of impurities in the uranium units used in this experiment.

The above mentioned benchmark evaluations contain a table of impurities typical for HEU parts from Y-12 that were carefully cast and machined in a similar manner to those used in the GROTESQUE experiments. [HEU-MET-FAST-069](#) indicates that impurity measurements are the average of 11 different spectrographic analyses of randomly sampled components for each impurity. These values are consistent with the nominal impurity content of highly enriched uranium metal at the Oak Ridge Y-12 Plant at the time the units were produced (i.e., the Y-12 enrichment and fabrication process typically produced 99.95 g of U per 100 g of metal). Oxygen and nitrogen content was assumed by the experimentalist to be 20 and 30 ppm, respectively, consistent with highly enriched uranium produced at the time of these experiments. The impurity data were taken from [HEU-MET-FAST-069](#) and are shown in Table 2.11.

HEU-MET-FAST-081

Those impurities listed as less than a minimum value are considered less than the detection limit, and the actual content is selected as half the detection limit and the other half representing the 1σ uncertainty.

Table 2.11. Typical HEU Impurities.^(a)

Element ^(a)	PPM by Weight ^(b)	Variation (ppm)	Standard Deviation (ppm) ^(c)
Ag	8	3-25	3.2
Ba	< 0.01 ^(d)	-	0.005
Bi	164	81-311	52.9
C	< 10	-	2.4
Ca	0.1	-	0.05
Cd	< 1	-	0.5
Co	5	2-15	1.9
Cr	7	4-12	1.9
Cu	25	10-40	8
K	< 0.2	0.2-0.8	0.1
Li	< 2	-	1
Mg	3	2-3	1.7
Mn	56	25-89	17.1
Mo	< 1	< 1 – 1	0.5
Na	27	15-50	7.7
Ni	100	-	10
Sb	38	10-80	17.4
Ti	1	-	0.5

- (a) Mass spectrographic analysis, except for oxygen and nitrogen, were taken from: J. T. Mihalcz, "Graphite and Polyethylene Reflected Uranium-Metal Cylinders and Annuli," Union Carbide Corporation Nuclear Division, Oak Ridge Y-12 Plant, Y-DR-81 (April 28, 1972). Oxygen and nitrogen content were assumed by the principal experimentalist to be 20 and 30 ppm, respectively. Minor differences in the impurities exist between values listed in Table 5 and the impurity values provided in [HEU-MET-FAST-051](#).
- (b) Except for the values shown as less than the detection limit, impurity data are average values from 11 randomly sampled uranium parts.
- (c) Personal communication, J. A. Mullens to John Mihalcz in [HEU-MET-FAST-076](#), June 2004.
- (d) Less than (<) indicates lower detection limit and not that the impurity is not present.

The average impurity content was increased by 3σ to find an upper perturbed k_{eff} value and subsequently decreased to find a lower perturbed k_{eff} value, although impurity content was not reduced below zero. Half the difference between the upper and lower perturbation k_{eff} values was used to represent the 3σ uncertainty variation in k_{eff} due to impurities in the HEU. Additionally, the weight fraction of the uranium metal was adjusted, as appropriate, to compensate for the adjustments in impurity content. A 1σ uncertainty of ± 5 ppm was assumed for the oxygen and nitrogen content. Results are shown in Table 2.12.

HEU-MET-FAST-081

Table 2.12. Uranium Impurities Uncertainty.

Deviation	Δk	\pm	$\sigma_{\Delta k}$	Scaling Factor	$\Delta k_{\text{eff}} (1\sigma)$	\pm	$\sigma_{\Delta k_{\text{eff}}}$
$\pm 3\sigma$	-0.00014	\pm	0.00001	3	-0.00005	\pm	<0.00001

2.2.10 HEU Spatial Variation – The radial placement of the 8 units of uranium on the diaphragm was measured to within 0.010 in. (0.0254 cm)^a and the deflection of each unit was measured to within 0.005 in. (0.0127 cm). The centerpiece was moved separately from the other 8 units because it is physically realistic to assume that the placement of the centerpiece was not dependent on the positioning of the other HEU units. Calculations were performed for five different variations in the spatial positioning of the nine metal units. Calculations were deemed unnecessary for three additional variations in the spatial positioning of the HEU units. Results are tabulated in Table 2.13. All uncertainties in the spatial placement and orientation of the HEU units were considered to represent 1 σ uncertainties.

Radial Position: Using the benchmark model to simulate the experiment, the 8 outer units were moved away from the centerpiece by 0.010 in. (0.0254 cm) to create an upper perturbation limit, and then moved the same distance closer to create a lower perturbation limit; the difference between the two limits was divided by two. As discussed in Section 2.2.1, due to the unique worths of each component, there is no reduction in the calculated uncertainty for correlated effects. Thus this uncertainty is treated as 100% systematic.

Angular Placement: No uncertainty is assessed for the angular placement of the eight units surrounding the centerpiece (as shown in Figure 1.13). The uncertainty is judged to be negligible compared to the uncertainty in k_{eff} due to the uncertainty in the radial distance of the units from the experiment center.

Vertical Deflection: The eight outer units were raised and then lowered by ± 0.005 in. (0.0127 cm) to determine an upper and lower perturbation limit for the uncertainty in their deflection. The difference between these two perturbations were divided by two.

Alternating Vertical Deflection: The 8 outer units were arranged in an alternating pattern of increased and decreased deflection height of ± 0.005 in. (0.0127 cm). The effect was negligible.

Centerpiece Vertical Deflection: To evaluate the vertical spatial variation of the centerpiece, it was raised and lowered by 0.005 in (0.0127 cm), creating an upper and lower perturbation limit, respectively, and the difference between the upper and lower perturbation k_{eff} values was divided by two.

Centerpiece Position: The radial placement was evaluated by moving the centerpiece 0.005 in. (0.0127 cm), which is half the radial position uncertainty of 0.010 in. (0.0254 cm), in positive and negative directions along the x- and y-axis. The largest change occurred when moving the centerpiece towards Unit 5. This value was selected to represent the uncertainty in the centerpiece placement.

Stack Order: The exact location of every individual piece in all nine HEU units is unknown. Any uncertainty due to the order of piece placement is considered negligible as most of the pieces have similar densities and isotopic abundances. Furthermore, the units are homogenized as the effective bias in neglecting gaps between parts is negligible. The simplification biases of using a single HEU density, a single uranium isotopic composition, and removing the holes in the cylinders are also small (Section 3.1).

Stack Alignment: Careful precision was typically used in ORCEF experiments performed with the vertical lift assembly, where the uncertainty in piece alignment within a stack was limited to within the

^a Personal communication with John T. Mihalzco, April 2011.

HEU-MET-FAST-081

manufacturing tolerances of the pieces (see [HEU-MET-FAST-069](#)). Therefore, it is concluded that additional uncertainty due to the alignment of pieces stacked within a unit would be negligible and already included in the evaluation of uncertainty in the HEU dimensions.

Table 2.13. HEU Spatial Variation.

Parameter Variation	Deviation	Δk	\pm	$\sigma_{\Delta k}$	Scaling Factor	$\Delta k_{\text{eff}} (1\sigma)$	\pm	$\sigma_{\Delta k_{\text{eff}}}$
Radial Coordinates	± 0.0254 cm	-0.00080	\pm	0.00001	1	-0.00080	\pm	0.00001
Vertical Deflection	± 0.0127 cm	-0.00003	\pm	0.00001	1	-0.00003	\pm	0.00001
Alternating Vertical Heights	± 0.0127 cm	0.00004	\pm	0.00001	1	0.00004	\pm	0.00001
Centerpiece Vertical Deflection	± 0.0127 cm	<0.00001	\pm	0.00001	1	<0.00001	\pm	0.00001
Centerpiece Position	± 0.0254 cm	-0.00008	\pm	0.00001	1	-0.00008	\pm	0.00001

2.3 Support Structure Worth

The measurements in the logbook detail the method used to determine the worth of the support structure for the experiment. The combined worth of the support plate, diaphragm, support ring, and support stand was determined to be $+10.2 \text{ } \phi^a$ using positive stable reactor period measurements.

Using the MCNP-calculated β_{eff} for this experiment of 0.0067, the equivalent k_{eff} value for the $10.2 \text{ } \phi$ worth of the support structures is $(0.0067 \times 0.102 \$) = +0.00068 \Delta k_{\text{eff}}$. There was an additional measurement using two 10 mil steel diaphragms, which has a worth of $19.29 \text{ } \phi$, demonstrating that the majority of the worth came from the diaphragm and not the other support structure components. Therefore the effect of neglecting the additional support structure would result in a negligible bias with no additional uncertainty.

It is typical to assume a 10% uncertainty in the worth measurements of the structure and diaphragm for this type of experiment performed at ORCEF, according to similar benchmark experiments performed by the same experimenter, [HEU-MET-FAST-059](#) and [HEU-MET-FAST-069](#). An uncertainty of 10% is typically larger than the uncertainty demonstrated when repeated worth measurements were performed for similar experiments. The uncertainty in the measurement of the support structure and β_{eff} is quantified in Table 2.14.

^a ORCEF Logbook 15r, p. 49.

Table 2.14. Support Structure Worth Uncertainty.

Parameter	Value	Uncertainty
Support Structure Worth (ρ)	+10.2	$\pm 10\%$
β_{eff}	0.0067	$\pm 5\%$
Reactivity (Δk_{eff})	+0.00068	± 0.00008

2.4 Room Return

Unreflected systems tend to be more sensitive to room return than those with reflection, so it was necessary to develop a simplified model of the ORCEF to estimate the effects of the surroundings on the experiment. The dimensions of the East Cell of the ORCEF are documented in other benchmarks, such as [HEU-MET-FAST-076](#). The uncertainty in the measurements of this facility was not available. Since the effect of room return is small, the uncertainty due to the room return itself is assumed to be negligible. The bias and bias uncertainty for removing the room from the model is evaluated further in Section 3.1.

2.5 Temperature

As indicated in Section 1.4, heating effects in the experiment components were negligible. A 1σ temperature variation of $\pm 2^\circ\text{C}$ sufficiently represents the temperature uncertainty in this experiment. Using a β_{eff} of 0.0067 and a temperature reactivity coefficient of $-0.3 \text{ } \rho/^\circ\text{C}$,^a the resulting Δk_{eff} is negligible (Table 2.15).

Table 2.15. Temperature Effect Uncertainty.

Deviation	$\Delta k_{\text{eff}} (1\sigma)$
$\pm 2^\circ\text{C}$	-0.00004

2.6 Measurement of k_{eff}

2.6.1 Initial Measurements – The experimental k_{eff} value was reported in the experimental logbook.^b This value was determined through stable reactor period measurements, and was reported in the reactivity unit of cents (ρ). As with the worth measurement of the support structure, a 10% uncertainty in the measured k_{eff} and a 5% uncertainty in β_{eff} is assumed. Table 2.16 contains the measured k_{eff} value in cents, and the reactivity value was converted into units of Δk using a calculated β_{eff} of 0.0067 to obtain the measured k_{eff} value.

^a Personal communication with John T. Mihalczko, March 2010.

^b ORCEF Logbook 15r, pp.47-48.

Table 2.16. Measured Reactivity Data.^(a)

Measurement Number	Measured Reactivity (ρ)	Measured Reactivity (Δk)	$k_{\text{eff}} \pm 1\sigma$
1	-9.20	-0.00062	0.99938 \pm 0.00007
2	-9.05	-0.00061	0.99939 \pm 0.00007
Average	-9.125	-0.00061	0.99939 \pm 0.00007

(a) Oak Ridge National Laboratory Critical Experiments Logbook 15r, p. 47.

2.6.2 Repeated Measurements – Repeatability measurements were also performed. The repeatability measurements are shown in Table 2.17. A 10% uncertainty in the measured k_{eff} and a 5% uncertainty in β_{eff} is assumed.

Table 2.17. Measured Repeatability Data.^(a)

Measurement Number	Measured Reactivity (ρ)	Measured Reactivity (Δk)	$k_{\text{eff}} \pm 1\sigma$
1	-7.87	-0.00053	0.99947 \pm 0.00006
2	-8.47	-0.00057	0.99943 \pm 0.00006
Average	-8.17	-0.00055	0.99945 \pm 0.00006

(a) Oak Ridge National Laboratory Critical Experiments Logbook 15r, p. 48. Labeled as “repeat of Experiment 4” from 6-15-64.

2.6.3 Experiment k_{eff} – The average of the four experimental measurements of k_{eff} are used to obtain the experiment k_{eff} value shown in Table 2.18.

Table 2.18. Experiment k_{eff} .

Average $k_{\text{eff}}^{(a)}$	Uncertainty $\sigma_{\Delta k_{\text{eff}}}$
0.99942	0.00003

2.7 Total Experimental Uncertainty

The total uncertainty for the experiment was calculated by taking the square root of the sum of the squares of all the individual uncertainties discussed in this section. The summarized total uncertainties for each case are presented in Table 2.19.

HEU-MET-FAST-081

Table 2.19. Total Experimental Uncertainty, Δk_{eff} .

Perturbed Parameter	Parameter Value	1 σ Uncertainty	$\pm\Delta k_{\text{eff}}$ (1 σ) ^(a)
Homogenization of Units	--	--	Negligible
Holes in Cylindrical Pieces	--	--	Negligible
Gaps between Pieces	--	--	Negligible
Total HEU Mass (g)	206522	28	Negligible
HEU Dimensions (cm)	Figures 1.2 – 1.10	Section 2.2.6	Negligible
Tilt Angle (°)	Table 2.7	0.068 / $\sqrt{2}$	0.00017
²³⁴ U Content (wt.%)	Table 2.9	0.05	Negligible
²³⁵ U Content (wt.%)	Table 2.9	0.05	Negligible
²³⁶ U Content (wt.%)	Table 2.9	0.05	Negligible
Impurity Content (wt.%)	Table 2.11		Negligible
Radial Position (cm)	Table 1.12	0.0254	0.00080
Angular Placement (°)	--	--	Negligible
Vertical Deflection (cm)	Table 2.7	0.0127	Negligible
Alternating Vertical Deflection (cm)	Table 2.7	0.0127	Negligible
Centerpiece Vertical Deflection (cm)	-1.755	0.0127	Negligible
Centerpiece (x, y) Position (cm)	(0, 0)	0.0127	Negligible
Stack Order	--	--	Negligible
Stack Alignment	--	--	Negligible
Support Structure Worth (ϵ) ^(b)	-10.2	1.14	Negligible
Room Return	--	--	Negligible
Temperature (K)	293	2	Negligible
Measurement of k_{eff} (ϵ) ^(b)	-9.13	0.72	Negligible
Experiment Repeatability (ϵ) ^(b)	-8.17	0.65	Negligible
Total Uncertainty	--	--	0.00082

(a) Uncertainties ≤ 0.00010 are considered negligible.

(b) Includes a 5% uncertainty in the β_{eff} value of 0.0067.

3.0 BENCHMARK SPECIFICATIONS

3.1 Description of the Model

The GROTESQUE experiment consisted of nine units comprised of smaller HEU pieces, eight of which were arranged in a circular manner on a steel diaphragm. The diaphragm had a hole cut in the center through which a ninth unit, the centerpiece, was raised to add reactivity. The weight of the eight units caused the diaphragm to sag, causing each unit to tilt slightly inward. The diaphragm, with its support structure, is not included in the benchmark model.

The original experiment was designed to test geometric capabilities when modeling complex arrangements. For this reason, including a detailed model in this evaluation is considered a preservation of the original intention of the work. However, there are several simplifications that can be applied to the model to create a simple version for other applications. For this reason, both simple and detailed models are developed in this section, with sample inputs for both models included in Appendix A. The simplifications used to create the models are described below and the corresponding biases are quantified. Please note that some simplifications were made to both models.

MCNP5 with ENDF/B-VII.0 cross section library data were used to evaluate biases in the benchmark models. A bias is considered negligible if Δk is ≤ 0.00010 .

3.1.1 Detailed Model -

3.1.1.1 HEU Simplifications – The pieces of each of the units have been homogenized into their respective basic units: rectangular parallelepipeds, cylinders, and a hemisphere. Small holes (support holes remnant from prior experimentation) in the cylindrical units were retained in the detailed model. The total mass of each unit was divided by the total unit volume to obtain unit densities (see Section 2.2.4). The effective bias in ignoring the gaps between pieces within a given unit was evaluated by approximating gaps between the pieces by twice the manufacturing tolerance of ± 0.002 in. (± 0.00508 cm). Actual gap thicknesses would be comparable to those found in [HEU-MET-FAST-051](#), which are considerably smaller in size than the tolerance value used in this evaluation.^a The number of pieces within a given unit is summarized in Table 2.5. Total unit mass was conserved. The effective bias was determined to be negligible. Uncertainty perturbations in mass and geometry of the HEU units was also negligible (Sections 2.2.5 and 2.2.6, respectively), supporting the negligibility of streaming effects due to minuscule gaps between individual pieces within each unit.

3.1.1.2 Support Structure Simplification – The experimenter measured the worth of removing the steel diaphragm and the other support structures as 10.2¢. The major support worth contribution came from the steel diaphragm. The experimentally measured model correction is $-0.00065 \pm 0.00007 \Delta k$ as discussed in Section 2.3. This correction applies to both simple and detailed models.

3.1.1.3 Room Return – The properties and dimensions of the room in which the experiment was performed were not provided in the references, but they are available in many other East Cell ORCEF experiment reports. The dimensions used in this evaluation were obtained from a similar benchmark report: [HEU-MET-FAST-076](#). The east cell is a 35×35×30 ft. high room, and the assemblies of uranium were located approximately 11.7 ft. from the five-foot-thick concrete west wall, 12.7 ft. from the two-foot-thick concrete north wall, and 9.2 ft. above the concrete floor. It was assumed that the unreported concrete wall, floor, and ceiling thicknesses are 5 ft.^b The concrete was modeled as Oak Ridge Concrete with a density of 2.3 g/cm³ and the room density of the air was assumed to be 1.2 kg/m³. The use of other types of concrete would provide similar results, as shown in [HEU-MET-FAST-076](#). Both

^a Personal communication with John T. Mihalcz, August 2011.

^b Personal communication with John T. Mihalcz, April 2011.

concretes were prepared using crushed limestone instead of sand due to the unavailability of sand at the time.^a

The consequences of neglecting the room return effects were estimated to be $-0.00099 \pm 0.00001 \Delta k_{\text{eff}}$. This worth is approximately equivalent to $-15.54 \pm 0.44 \text{ } \phi$, including an assumed 5% uncertainty in β_{eff} . This simplification was used in both the simple and detailed models.

3.1.1.4 Impurities – The exact impurity content of the GROTESQUE uranium was unknown. Impurity data were not provided, but similar experiments provided some insight into possible impurities and their contents (see Table 2.11). The average impurity content, as discussed in Section 2.2.9, was added to the model, and the uranium mass appropriately decreased, to evaluate the effective bias in neglecting impurities in the benchmark models. Modeling the experiment without the inclusion of possible impurities created a bias of $-0.00022 \pm 0.00003 \Delta k$. This simplification was used in both the simple and detailed models.

3.1.1.5 Bias Summary for the Detailed Model – Table 3.1 summarizes each individual bias discussed in Section 3.1.1. The total bias for the detailed benchmark model is the difference between the calculated k_{eff} value from a detailed model with impurities (excluding support structure and room return effects) and one incorporating the simplifications discussed in this section. This difference is added to the individual biases obtained for the experimentally determined removal of the support structure and estimated room return effects.

Table 3.1. Summary of Evaluated Biases for Detailed Model.

Bias Description	Bias $\pm 1\sigma$
Intra-Unit Gaps and Unit Mass Density	Negligible
Removal of Support Structures	-0.00068 ± 0.00008
Room Return	-0.00099 ± 0.00003
Removal of Impurities	-0.00022 ± 0.00003
Total Bias^(a)	-0.00189 ± 0.00009

- (a) The total bias for the detailed model was obtained by comparing the calculated eigenvalues of a model with and without impurities and adding the difference to the experimentally measured simplification of support structure removal and the estimated correction for room return effects.

3.1.2 Simple Model -

The geometrically detailed model from Section 3.1.1 was further simplified in order to make a simple benchmark model. The following simplifications have been incorporated into the simple model, in addition to the simplifications already included in the detailed model, as described above in Section 3.1.1.

3.1.2.1 Additional HEU Simplifications – The 0.254 cm radius holes in the HEU cylinders were removed from the model and the density was appropriately reduced (see Section 2.2.4). This created a bias of $-0.00018 \pm 0.00003 \Delta k$.

An average uranium density was calculated by dividing the total mass of the HEU components (206522 g) by the total volume. The effective bias in modeling all units with the same average density is $0.00053 \pm 0.00003 \Delta k$.

^a Personal communication with John T. Mihalcz, February 2010.

A mass-weighted average uranium content was calculated for this experiment (see Table 2.9). The effective bias in modeling all units with the same uranium content is $-0.00016 \pm 0.00003 \Delta k$.

The bottoms of all nine HEU units were modeled as if placed on a single planar surface. This necessitated raising the outer eight units between 0.087 and 0.290 cm. The centerpiece was raised by 1.755 cm. This created a bias of $0.00028 \pm 0.00003 \Delta k$.

The slight inward tilt of the eight outer units was removed. This caused a bias of $-0.00560 \pm 0.00003 \Delta k$. Due to the large, dominating, bias for removing the tilt of the units, the calculation was repeated for this bias using KENO-VI^a with ENDF/B-VII.0 (238-group) cross section data. The calculated bias for removing the unit tilt using KENO-VI was $-0.00623 \pm 0.00011 \Delta k$. Additional calculations using a developmental version of the MONK9^b Monte Carlo Program were performed. A calculation with MONK9(DEV) and ENDF/B-VII.0 obtained a result of $-0.00550 \pm 0.00014 \Delta k$.^c The standard deviation of these three values was used to obtain an estimated 1σ bias uncertainty of $\pm 0.00040 \Delta k$. Calculations using MONK9 also demonstrated that the bias was approximately the same, within statistical uncertainty, regardless of which neutron cross section library was used. Furthermore, the effective cumulative bias determined by removing the tilt from each individual unit and summing the results is approximately the same as the bias obtained when the tilt was simultaneously removed from all units.

3.1.2.2 Bias Summary for the Simple Model – Table 3.2 summarizes each individual bias discussed in Section 3.1.2, where the total bias for the simple benchmark model is the sum the difference between the calculated k_{eff} value from a detailed model with impurities (excluding support structure and room return effects) and one incorporating the simplifications discussed in this section and Section 3.1.1. This difference is added to the individual biases obtained for the experimentally determined removal of the support structure and estimated room return effects.

Correlating effects in bias analysis simplifications may also contribute to the difference between the summation of the individual biases and the bias calculated for the benchmark model when all simplifications are performed simultaneously. This difference, however, is within the estimated 3σ bias uncertainty. The bias computed with all simplifications included together is the best representative of the true bias. The uncertainty in that bias is obtained from the individual analysis of each simplification.

^a D. F. Hollenbach, L. M. Petrie, S. Goluoglu, N. F. Landers, and M. E. Dunn, "KENO-VI: A General Quadratic Version of the KENO Program," ORNL/TM-2005/39 Version 6 Vol. II, Sect. F17, Oak Ridge National Laboratory (January 2009).

^b M. J. Armishaw and A. J. Cooper, "Current Status and Future Direction of the MONK Software Package," *ICNC 2007*, St. Petersburg, Russia, May 28 – June 1 (2007).

^c Personal Communication with Dave Hanlon, July 2011.

Table 3.2. Summary of Evaluated Biases for Simplified Model.

Bias Description	Bias $\pm 1\sigma$
Intra-Unit Gaps and Unit Mass Density	Negligible
Removal of Support Structures	-0.00068 \pm 0.00008
Room Return	-0.00099 \pm 0.00003
Removal of Impurities	-0.00022 \pm 0.00003
Removal of Holes in Cylinders	-0.00018 \pm 0.00003
Average Fuel Density	+0.00053 \pm 0.00003
Average Uranium Isotopic Composition	-0.00016 \pm 0.00003
Placement of All Units on a Level Surface	+0.00028 \pm 0.00003
Removal of Unit Tilt	-0.00560 \pm 0.00040
Sum of Individual Biases	-0.00702 \pm 0.00041
Total Bias^(a)	-0.00768 \pm 0.00041

- (a) The total bias for the simple model was obtained by comparing the calculated eigenvalues of a model with and without the model simplifications discussed above and adding the difference to the experimentally measured simplification of support structure removal and the estimated bias for room return effect.

The total bias for both of the detailed and simple benchmark models is compared in Table 3.3.

Table 3.3. Total Model Bias (Δk).

Detailed Model	Simple Model
-0.00189 \pm 0.00009	-0.00768 \pm 0.00041

3.2 Model Dimensions

Both the detailed and simple benchmark models are described in this section.

3.2.1 Individual HEU Units – The following figures are not to scale with respect to each other. However, each individual figure shows the components of each unit to scale with respect to the other components of that unit.

The first major unit (Unit 1) is located on the south side of the experiment, along the y-axis. It is a complex parallelepiped, as shown in Figure 3.1. The height at the highest point is 13.377 cm (11.155 cm + 2.222 cm). The base parallelepiped is 12.703 cm along the x-axis, and 12.703 in the y direction. The smallest height is 11.155 cm. The dimensions of Unit 1 are identical for both the detailed and simple models.

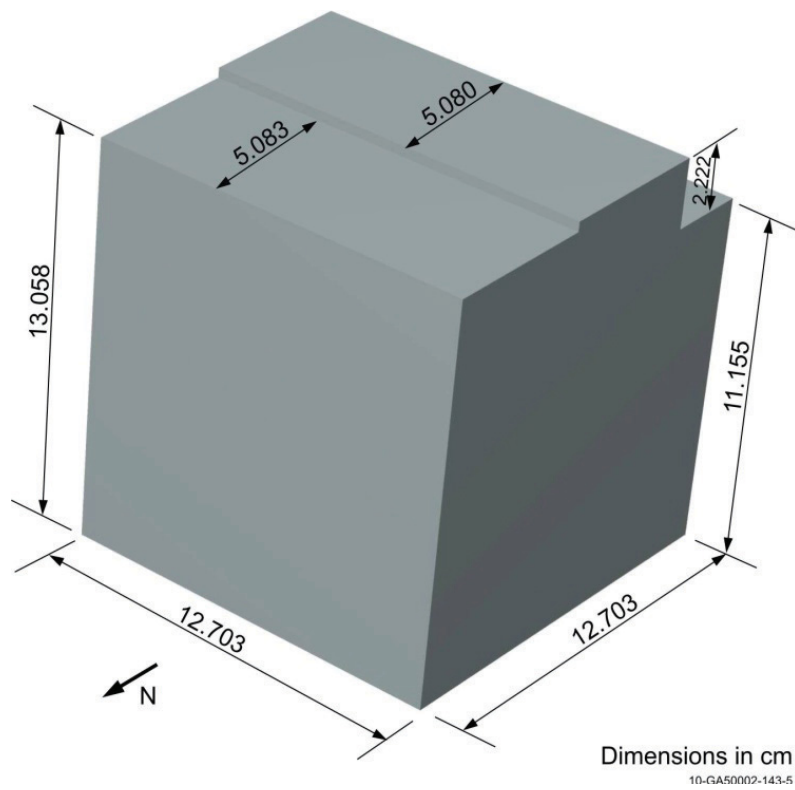


Figure 3.1. Unit 1 (detailed and simple model).

Unit 2 is the next unit to the west of Unit 1; subsequent units will continue to be described in a clockwise direction from Unit 1. Unit 2 is a cylinder with a diameter of 9.111 cm and a height of 12.918 cm. Figure 3.2 shows the cylinder used in the detailed model in the upper portion of the figure (top) and the simple model in the lower portion (bottom).

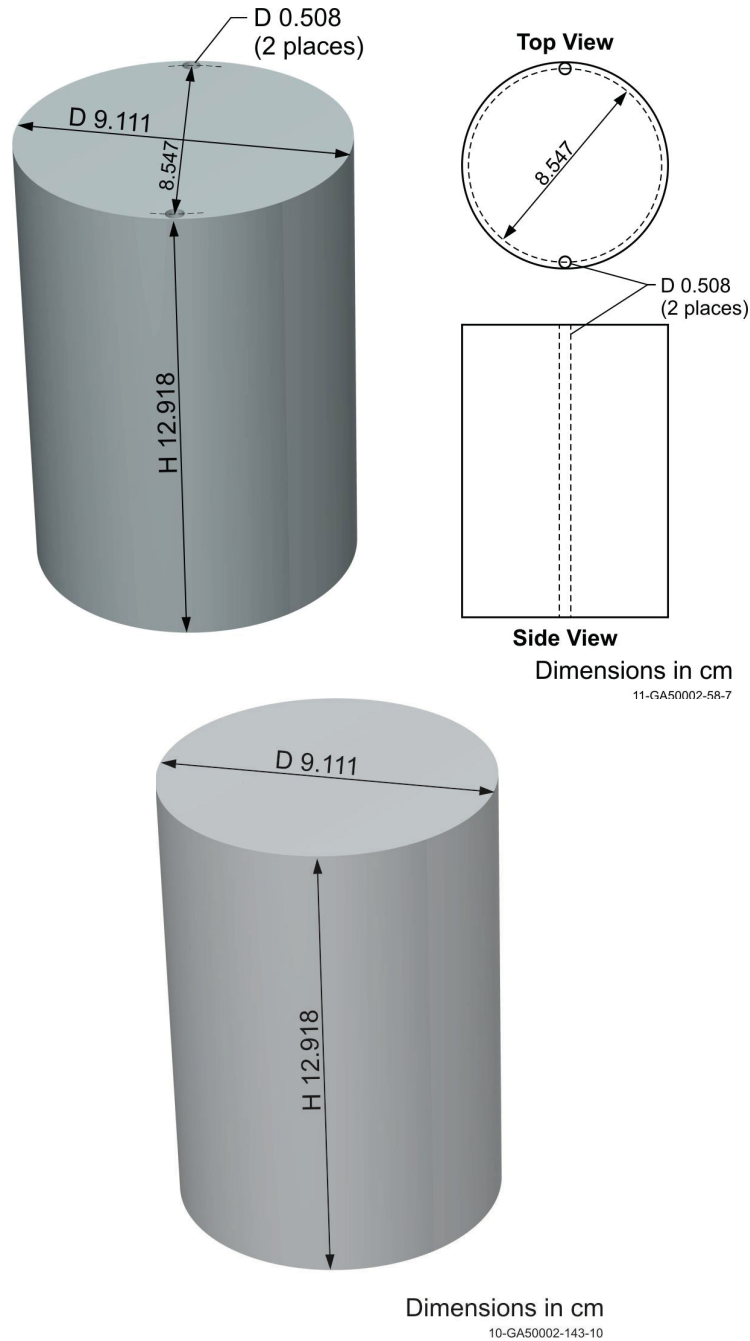


Figure 3.2. Unit 2 (top=detailed, bottom=simple).

Unit 3 is close to being aligned with the x-axis of the model, though not exactly centered on the axis. It is a cylinder with a diameter of 11.522 cm and a height of 13.475 cm. Figure 3.3 shows the cylinder used in the detailed model on the top and the simple model on the bottom.

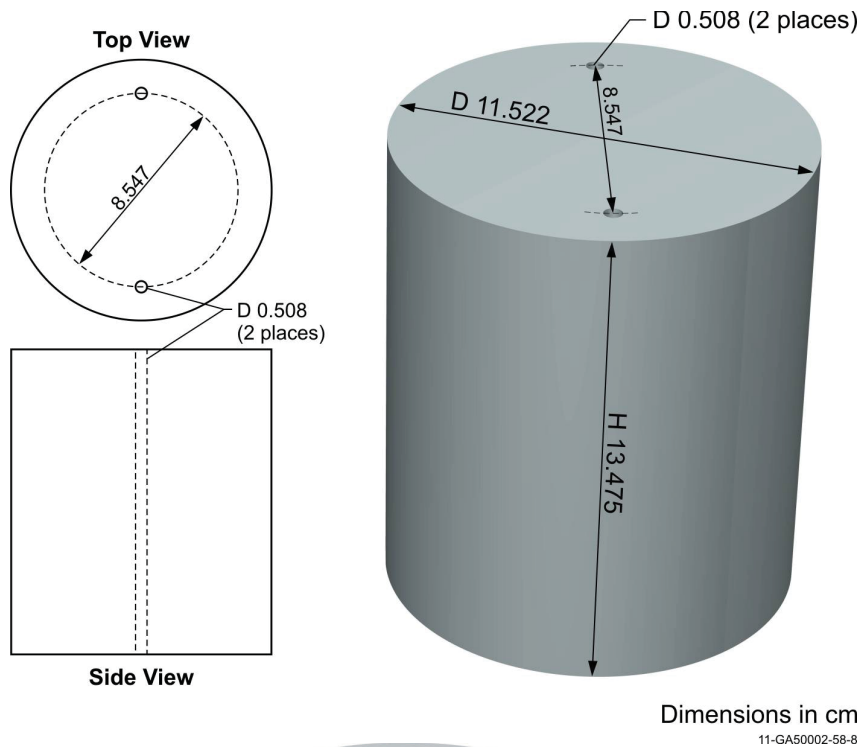


Figure 3.3. Unit 3 (top=detailed, bottom=simple).

Unit 4 is the last cylinder on the west side of the experiment. It is 9.105 cm in diameter and 12.969 cm high. Figure 3.4 shows the cylinder used in the detailed model on the top and the simple model on the bottom.

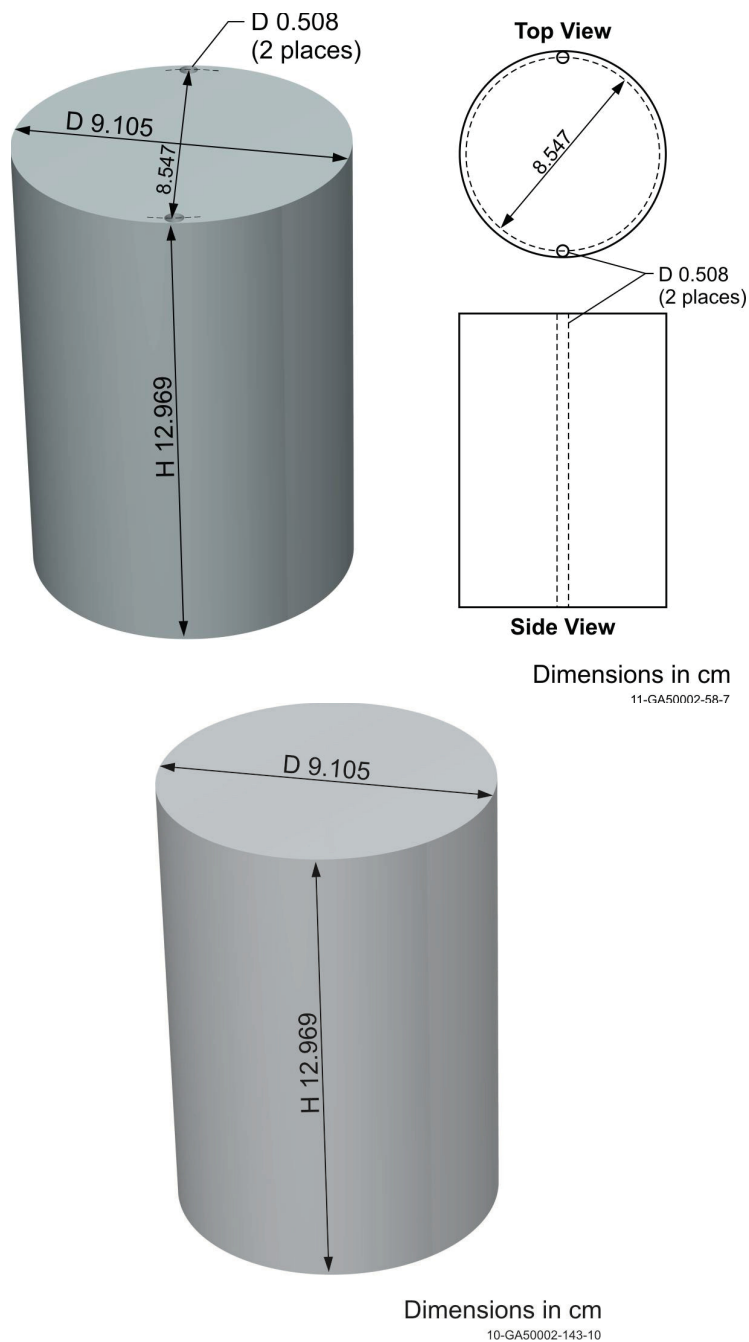


Figure 3.4. Unit 4 (top=detailed, bottom=simple).

Unit 5 is on the north side of the experiment and opposite Unit 1. It is composed of a rectangular parallelepiped with a cylinder placed on top. The cylinder is positioned on the half of the parallelepiped closest to the center of the experiment. The parallelepiped is $12.703 \times 7.620 \times 8.910$ cm and aligned with the longest side parallel to the y-axis. The cylinder on top is 9.146 cm in diameter and 4.319 cm in height. Figure 3.5 shows the unit used in the detailed model on the top and the simple model on the bottom.

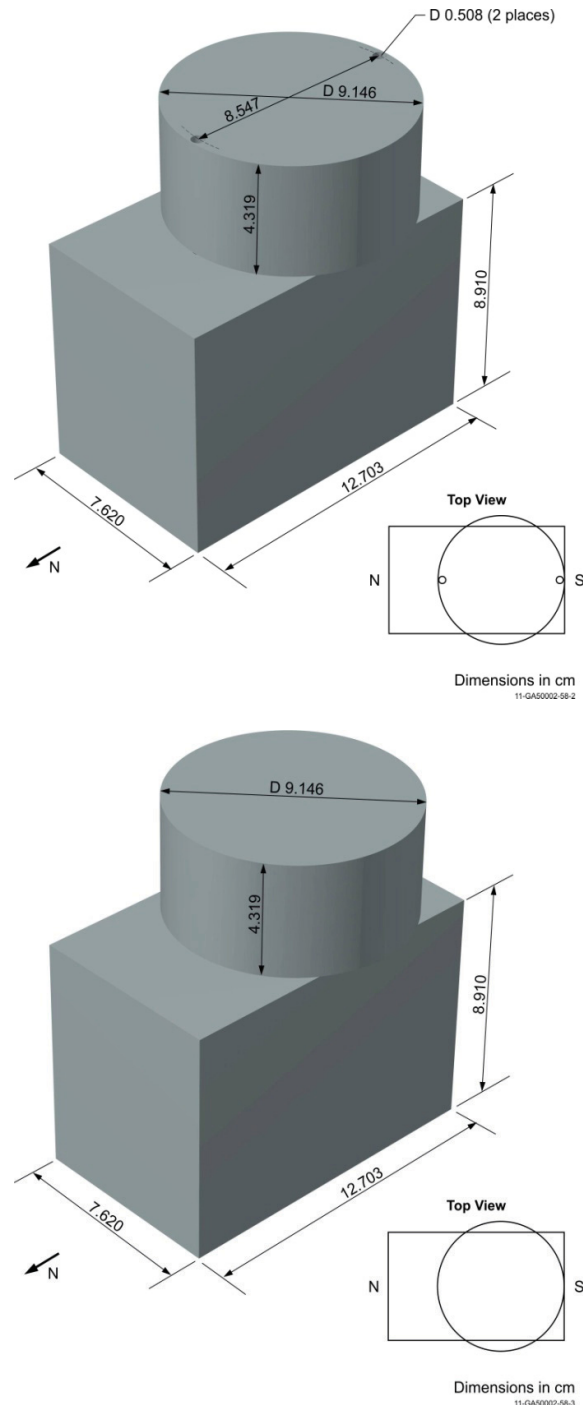


Figure 3.5. Unit 5 (top=detailed, bottom=simple).

Units 6, 7, and 8 are positioned on the east side of the circular experiment. They are all cylinders of differing dimensions. Unit 6 (Figure 3.6) has a diameter of 9.109 and a height of 12.974. Unit 7 (Figure 3.7) is very nearly aligned with the x-axis of the experiment, but not completely centered on the axis. It is 11.499 cm in diameter and the height is 13.475 cm. Unit 8 (Figure 3.8) is the last cylinder in the experiment, counting clockwise from Unit 1. It is 9.113 cm in diameter and the height is 12.954 cm. In each of Figures 3.6 through 3.8, the cylinder used in the detailed model is shown on the top and the simple model on the bottom.

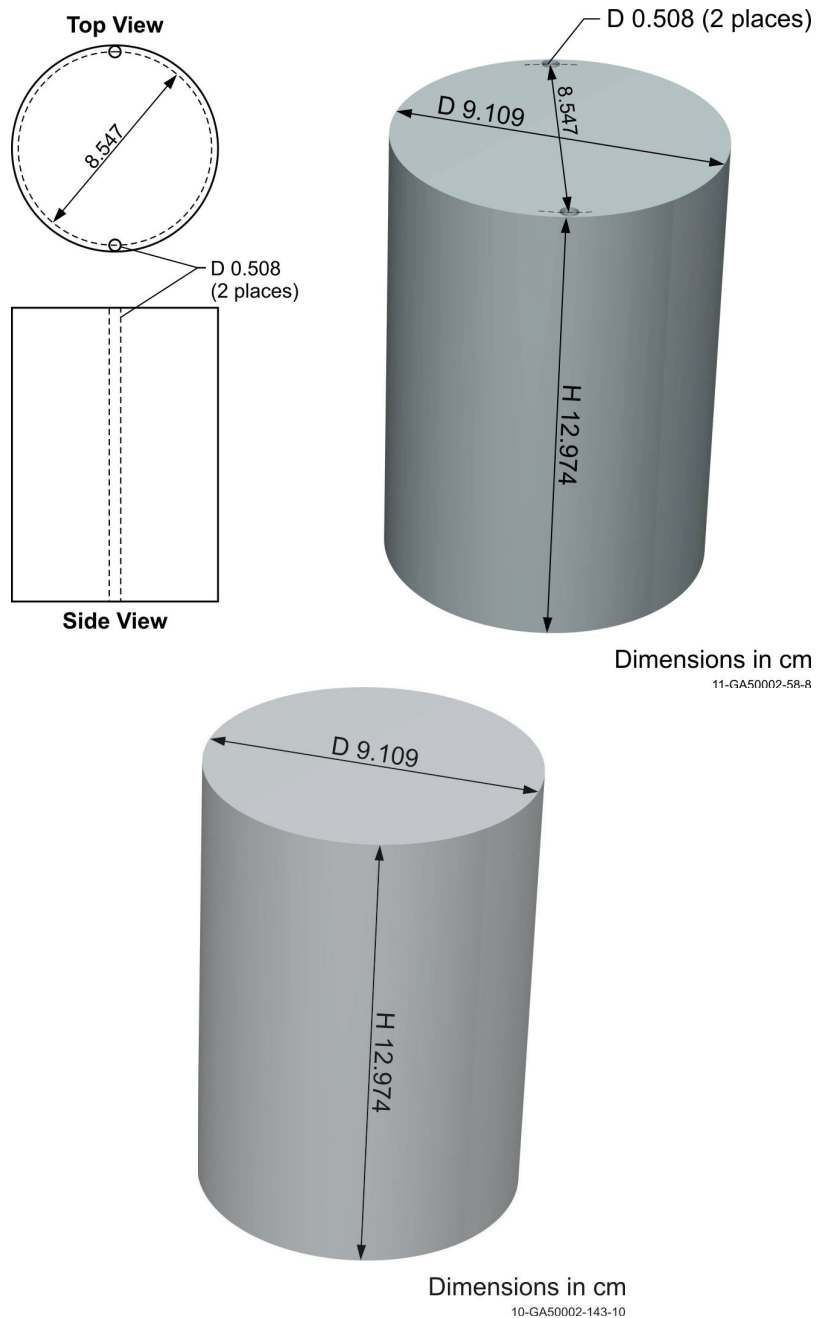
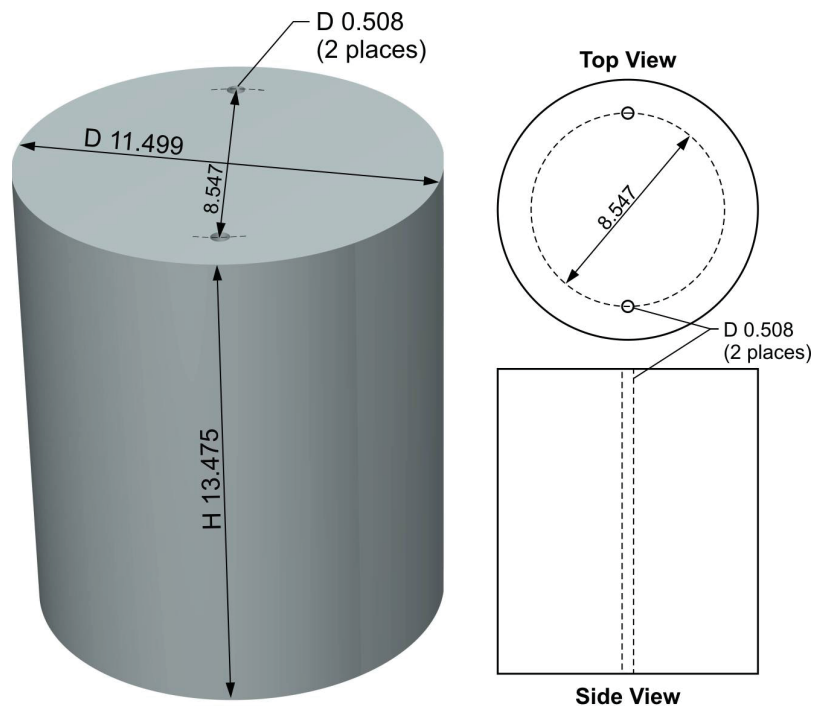
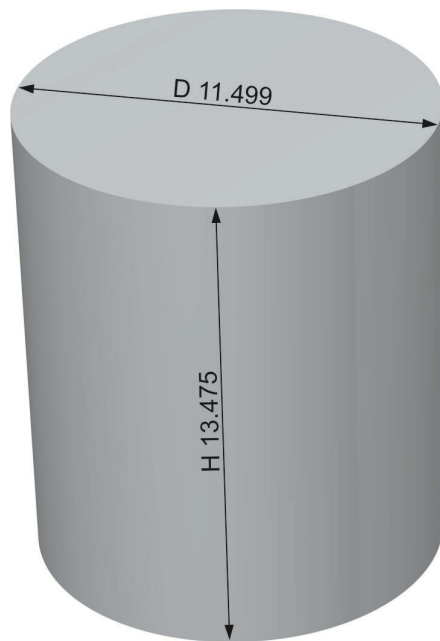


Figure 3.6. Unit 6 (top=detailed, bottom=simple).

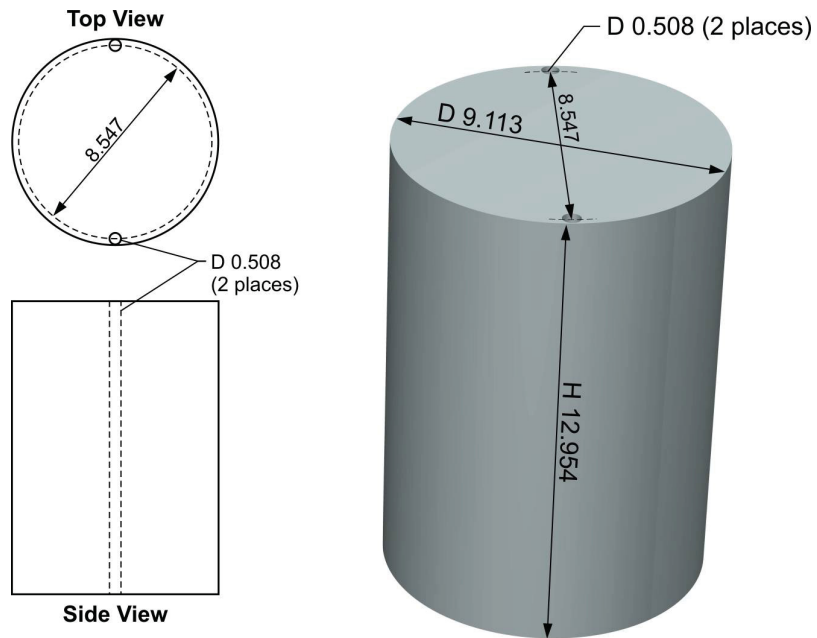


Dimensions in cm
11-GA50002-58-7

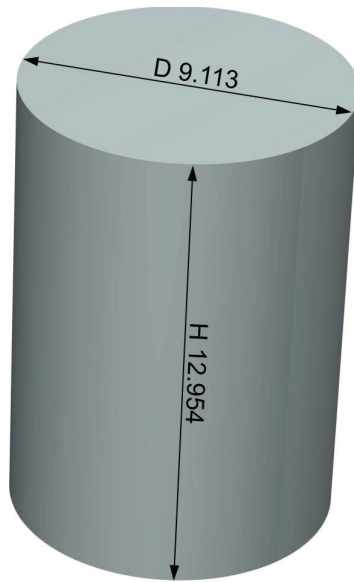


Dimensions in cm
10-GA50002-143-10

Figure 3.7. Unit 7 (top=detailed, bottom=simple).



Dimensions in cm
11-GA50002-58-8



Dimensions in cm
11-GA50002-48-10

Figure 3.8. Unit 8 (top=detailed, bottom=simple).

Unit 9 is the centerpiece of the experiment. It is composed of a hemisphere, a cylinder, and a rectangular parallelepiped. The cylinder is the bottommost piece, with a diameter of 11.514 cm and a height of 2.692 cm. The rectangular parallelepiped was placed on top of the cylinder, with the west and south edges flush with the outer most point of the cylinder on the west and south sides. This created an un-centered effect, with the overhangs in the east and north directions of the experiment. The parallelepiped was 12.700 cm \times 12.700 cm and 5.718 cm in height. The hemisphere is the uppermost part, with the outer most point of its west edge flush with the west edge of the other two pieces but with the north edge flush with the north side of the parallelepiped. It is 12.164 cm in diameter, and so does not extend fully to the opposite side of the parallelepiped. This unit is illustrated in detail in Figure 3.9, the unit used in the detailed model is on the top and the simple model on the bottom.

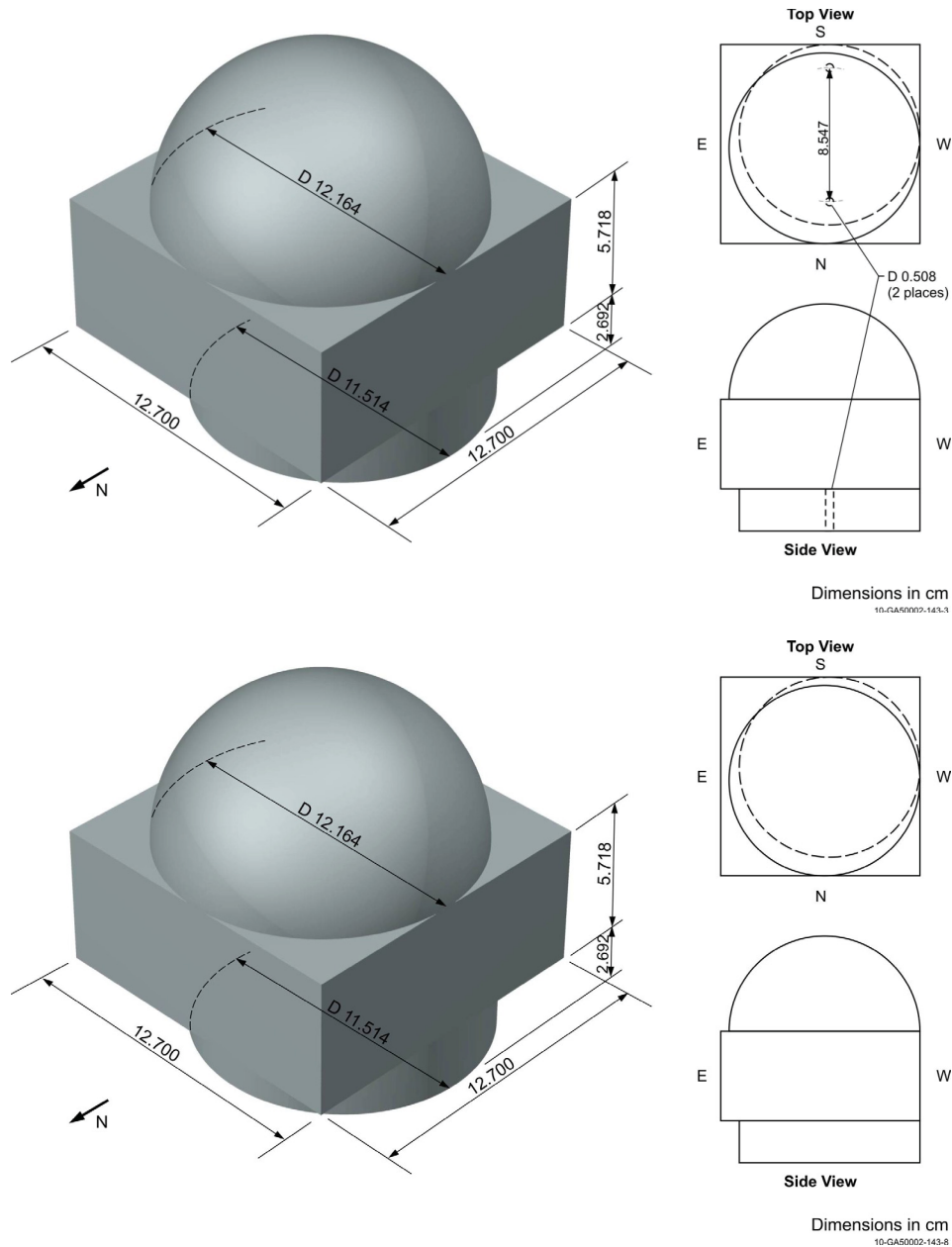


Figure 3.9. Unit 9, Centerpiece(top=detailed, bottom=simple).

3.2.2 Assembly Description – The exact position of the center of the bottom of each major unit in relation to the center of the experimental configuration is described in Table 3.4. This information is used for both the simple and detailed models. Additional information regarding the vertical positioning of the pieces and their tilt angle towards the center of the experiment, necessary for describing the detailed model, are provided in Table 3.5. The simple model does not have tilting and all pieces are modeled as if supported on a level planar surface. Figures 3.10 and 3.11 show an isometric and schematic view of the simple model, respectively, to demonstrate placement of units within the simple and detailed models. Only the simple model is shown because the overall placement of the units is the same in both models. The tilt, bottom z coordinate, and holes in the cylinders removed from the simple model (See Section 3.1.2) are not shown because they do not affect the overall macroscopic dimensions being presented in the following tables and figures.

Table 3.4. Assembly Geometry Positioning.

Unit Number	Angular Spacing (°)	Center Bottom X Coordinate (cm)	Center Bottom Y Coordinate (cm)
1	270.0	0.0	-17.464
2	217.5	-12.176	-9.343
3	173.5	-16.333	1.861
4	130.5	-9.539	11.168
5 ^(a)	90.0	0.0	17.477
5 ^(b)	90.0	0.0	15.698
6	48.0	9.854	10.944
7	5.0	16.388	1.434
8	322.0	12.029	-9.398
9 ^(b)	-	-0.593	-0.593
9 ^(a)	-	0.0	0.0
9 ^(c)	-	-0.268	0.268

(a) Rectangular parallelepiped component piece.

(b) Cylinder component piece.

(c) Hemisphere component piece.

Table 3.5. Vertical Positioning and Tilt Angle
for HEU Units (detailed model only).

Unit Number	Bottom Z Coordinate (cm)	Tilt Angle (°)
1	0.150	1.350
2	0.111	1.400
3	0.174	1.173
4	0.156	1.970
5 ^(a)	0.290	2.580
5 ^(b)	9.2	2.580
6	0.134	1.680
7	0.140	1.400
8	0.087	1.100
9 ^(b)	-1.755	0.000
9 ^(a)	0.937	0.000
9 ^(c)	6.655	0.000

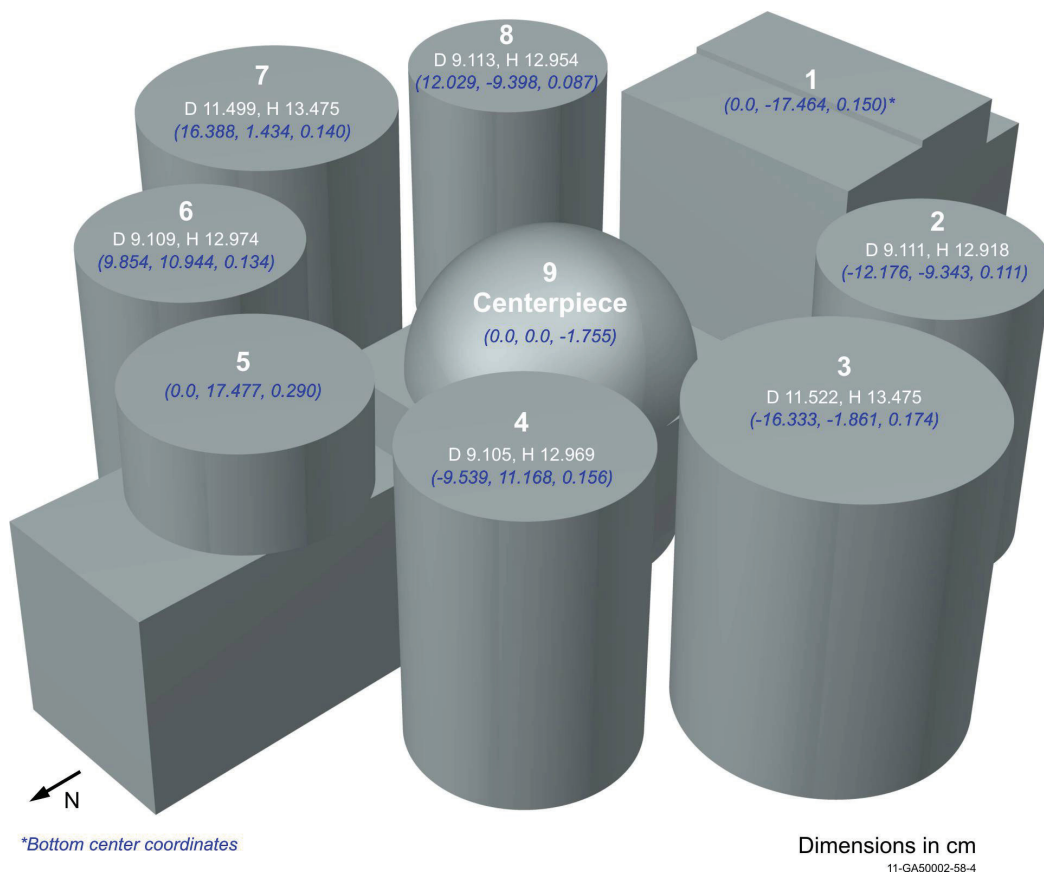


Figure 3.10. Isometric View of the GROTESQUE Models.
(Holes in cylindrical pieces not shown).

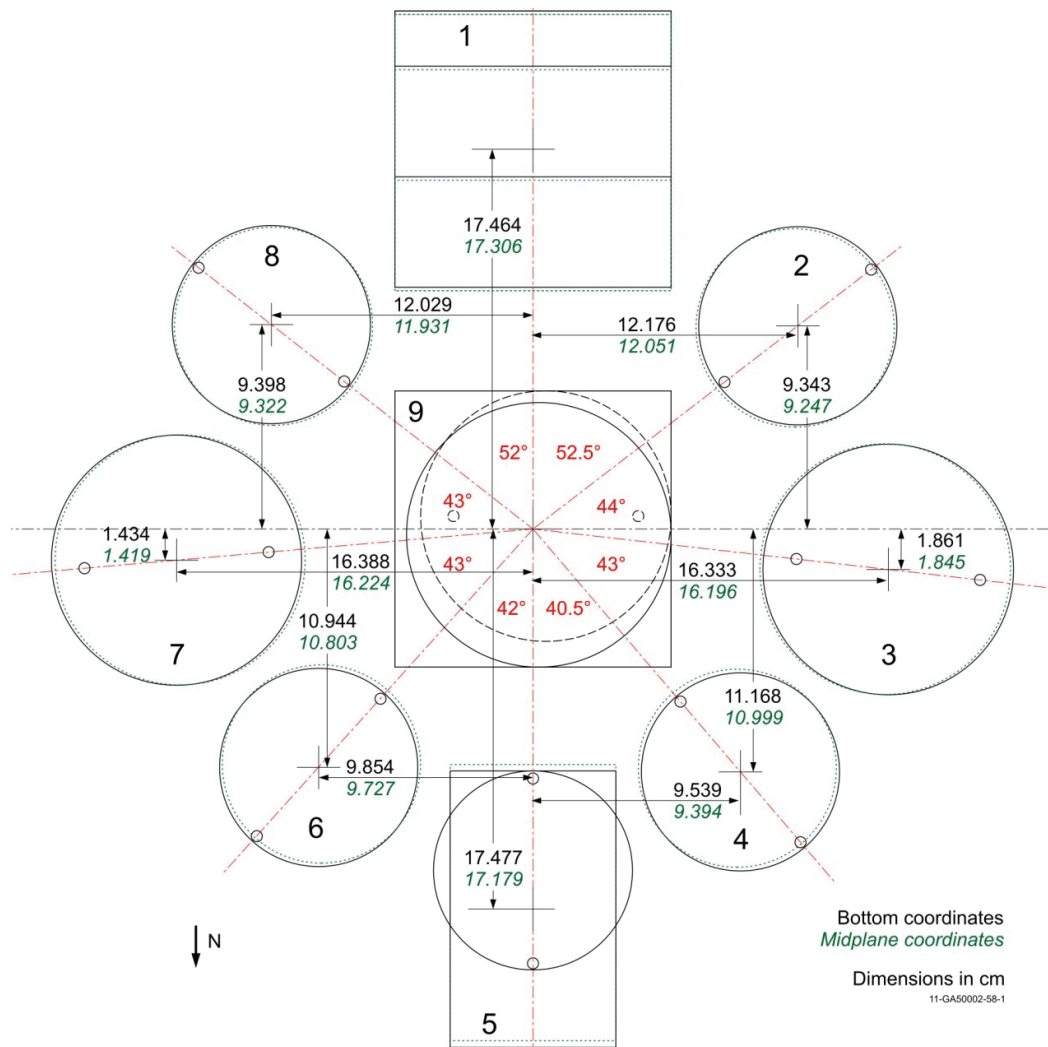


Figure 3.11. Schematic View of the GROTESQUE Models (Top View).

3.3 Description of Material Data

3.3.1 HEU Metal – The atomic densities of uranium isotopes are provided in Table 3.6 and Table 3.7 for the detailed and simple models, respectively. Each unit (or subunit in the case of Units 5 and 9) have unique compositions and densities in the detailed model. All units have the same density and isotopic composition in the simple model. The atom densities for both models have been adjusted for the removal of impurities; the effective uranium content fraction is 0.99951.

Table 3.6. Detailed Model Uranium Composition.

Unit	Isotope	Composition (wt.%)	Atom Density (atoms/b- cm)
1	²³⁴ U	1.07	5.1270E-04
	²³⁵ U	93.15	4.4443E-02
	²³⁶ U	0.68	3.2306E-04
	²³⁸ U	5.10	2.4025E-03
2	²³⁴ U	0.97	4.6998E-04
	²³⁵ U	93.15	4.4940E-02
	²³⁶ U	0.24	1.1530E-04
	²³⁸ U	5.64	2.6867E-03
3	²³⁴ U	0.97	4.6730E-04
	²³⁵ U	93.15	4.4684E-02
	²³⁶ U	0.24	1.1464E-04
	²³⁸ U	5.64	2.6713E-03
4	²³⁴ U	0.97	4.6733E-04
	²³⁵ U	93.15	4.4687E-02
	²³⁶ U	0.24	1.1465E-04
	²³⁸ U	5.64	2.6715E-03
5 – box	²³⁴ U	1.07	5.1364E-04
	²³⁵ U	93.15	4.4525E-02
	²³⁶ U	0.68	3.2365E-04
	²³⁸ U	5.10	2.4070E-03
5 – cylinder	²³⁴ U	0.97	4.6762E-04
	²³⁵ U	93.15	4.4714E-02
	²³⁶ U	0.24	1.1472E-04
	²³⁸ U	5.64	2.6731E-03
6	²³⁴ U	0.97	4.6694E-04
	²³⁵ U	93.15	4.4650E-02
	²³⁶ U	0.24	1.1455E-04
	²³⁸ U	5.64	2.6693E-03
7	²³⁴ U	0.97	4.6818E-04
	²³⁵ U	93.15	4.4768E-02
	²³⁶ U	0.24	1.1485E-04
	²³⁸ U	5.64	2.6763E-03
8	²³⁴ U	0.97	4.6808E-04
	²³⁵ U	93.15	4.4759E-02
	²³⁶ U	0.24	1.1483E-04
	²³⁸ U	5.64	2.6758E-03
9 – cylinder	²³⁴ U	0.97	4.6881E-04
	²³⁵ U	93.15	4.4829E-02
	²³⁶ U	0.24	1.1501E-04
	²³⁸ U	5.64	2.6800E-03
9 – box	²³⁴ U	1.07	5.1352E-04
	²³⁵ U	93.15	4.4514E-02
	²³⁶ U	0.68	3.2358E-04
	²³⁸ U	5.10	2.4064E-03
9 – hemisphere	²³⁴ U	0.97	4.6792E-04
	²³⁵ U	93.15	4.4743E-02
	²³⁶ U	0.24	1.1479E-04
	²³⁸ U	5.64	2.6749E-03

Table 3.7. Simple Model Uranium Composition.

Isotope	Composition (wt.%)	Atom Density (atoms/b- cm)
²³⁴ U	1.00	4.7990E-04
²³⁵ U	93.15	4.4512E-02
²³⁶ U	0.39	1.8557E-04
²³⁸ U	5.46	2.5761E-03

3.4 Temperature Data

The benchmark model is evaluated at room temperature (293 K) for both the simple and detailed models.

3.5 Experimental and Benchmark Model k_{eff}

The experimental and benchmark k_{eff} values for GROTESQUE are presented in Table 3.8 with their associated uncertainties. The reactivity effects of the support structure, room return effects, and biases discussed in Section 3.1 have been added to the experimental k_{eff} to obtain the benchmark k_{eff} values for both the detailed and simplified benchmark models. The experimental uncertainty was evaluated in Section 2 and summarized in Table 2.19. The experimental uncertainty is combined in quadrature with the bias uncertainty to obtain the total benchmark model uncertainty.

Table 3.8. Experimental and Benchmark k_{eff} Values (1σ).

Model	Experimental k_{eff}	Δk Bias	Benchmark k_{eff}
Detailed	0.9994 ± 0.0008	-0.0019 ± 0.0001	0.9975 ± 0.0008
Simple		-0.0077 ± 0.0004	0.9917 ± 0.0009

4.0 RESULTS OF SAMPLE CALCULATIONS

Results were calculated using MCNP5-1.51 with ENDF/B-VII.0, ENDF/B-VI.8,^a ENDF/B-V.2,^b and JENDL-3.3^c neutron cross-section libraries (see Tables 4.1 and 4.2 for the detailed and simple models, respectively) with example input listings and specifications provided in Appendix A. The MCNP5 calculations were performed with 1,050 generations that included 1,000,000 neutrons per generation. The k_{eff} estimates did not include the first 50 generations. The statistical uncertainty in k_{eff} is ± 0.00002 (1σ) in all cases. Eigenvalues calculated with MCNP5 are over 3σ lower than the benchmark values; the reason for this computational bias is unknown.

Calculations were also performed using KENO-VI (SCALE 6.0) with ENDF/B-VII.0, ENDF/B-VI.8, and ENDF/B-V.2 neutron cross-section libraries. The KENO-VI calculations were performed with 1,050 generations that included 100,000 neutrons per generation. The k_{eff} estimates did not include the first 50 generations. The statistical uncertainty in k_{eff} is approximately ± 0.00008 (1σ). These results are also provided in Tables 4.1 and 4.2 for the detailed and simple models, respectively. Eigenvalues calculated with KENO-VI are approximately 3σ greater than the benchmark values; the reason for the large difference between the MCNP5 and KENO-VI calculated results, using the same cross section data, is unknown.

Calculations were provided by Serco using a developmental version of MONK^d with JEF2.2,^e JEFF3.1,^f ENDF/B-VII.0, or CENDL-3.1^g based BINGO continuous energy cross section libraries. The MONK9(DEV) calculations employed 5,000 superhistories per stage with up to 10 neutron generations tracked per superhistory, and was run for 10 settling stages followed by approximately 70 stages, to achieve a prevision of 0.0005. The calculations were repeated twenty-five times each to achieve a prevision of ± 0.0001 . The MONK calculations with ENDF/B-VII.0 are in good agreement with the MCNP results. Calculations with MONK and CENDL-3.1 provide calculated k_{eff} values closest to the benchmark values.

^a H. D. Lemmel, P. K. McLaughlin, and V. G. Pronyaev, "ENDF/B-VI Release 8 (Last Release of ENDF/B-VI) the U.S. Evaluated Nuclear Data Library for Neutron Reaction Data," IAEA-NDS-100 Rev. 11, International Atomic Energy Agency, Vienna (November 2001).

^b B. A. Magurno and P. G. Young, "ENDF-201 Supplement I, ENDF/B-V.2 Summary Documentation," BNL-NCS-17541, Brookhaven National Laboratory (January 1985).

^c K. Shibata, et al., "Japanese Evaluated Nuclear Data Library Version 3 Revision3: JENDL-3.3," *J. Nucl. Sci. Tech.*, **39**: 1125-1136 (November 2002).

^d Personal Communication with Dave Hanlon, July 2011.

^e "The JEF-2.2 Nuclear Data Library," JEFF Report 17, Organisation for Economic Co-operation and Development, Paris, France (2000).

^f A. Koning, R. Forrest, M. Kellett, R. Mills, H. Henriksson, and Y. Rugama, "The JEFF-3.1 Nuclear Data Library," JEFF Report 21, Organisation for Economic Co-operation and Development, Paris, France (2006).

^g Z. G. Ge, et al., "The Updated Version of Chinese Evaluated Nuclear Data Library (CENDL-3.1)," *Proc. Int. Conf. Nucl. Data for Sci. Tech.*, Jeju Island, Korea, April 26-30 (2010).

Table 4.1. Sample Calculation Results for the Detailed Benchmark Model.

Analysis Code	Neutron Cross Section Library	Calculated			Benchmark			$\frac{C-E}{E}(\%)$
		k_{eff}	\pm	σ	k_{eff}	\pm	σ	
MCNP5	ENDF/B-VII.0	0.99391	\pm	0.00002	0.9975	\pm	0.0009	-0.36
	ENDF/B-VI.8	0.99090	\pm	0.00002				-0.66
	ENDF/B-V.2	0.99462	\pm	0.00002				-0.29
	JENDL-3.3	0.99222	\pm	0.00002				-0.53
KENO-VI	ENDF/B-VII.0 (continuous energy)	1.00133	\pm	0.00008				0.38
	ENDF/B-VII.0 (238-group)	1.00116	\pm	0.00007				0.31
	ENDF/B-VI.8 (238-group)	0.99814	\pm	0.00009				0.06
	ENDF/B-V.2 (238-group)	1.00141	\pm	0.00009				0.39
MONK9(DEV) ^(a)	JEF-2.2	0.9899	\pm	0.0001				-0.76
	JEFF-3.1	0.9914	\pm	0.0001				-0.61
	ENDF/B-VII.0	0.9943	\pm	0.0001				-0.32
	CENDL-3.1	0.9953	\pm	0.0001				-0.22

(a) Results provided by Dave Hanlon from Serco in the United Kingdom.

Table 4.2. Sample Calculation Results for the Simple Benchmark Model.

Analysis Code	Neutron Cross Section Library	Calculated			Benchmark			$\frac{C-E}{E}(\%)$
		k_{eff}	\pm	σ	k_{eff}	\pm	σ	
MCNP5	ENDF/B-VII.0	0.98810	\pm	0.00002	0.9917	\pm	0.0010	-0.37
	ENDF/B-VI.8	0.98507	\pm	0.00002				-0.67
	ENDF/B-V.2	0.98877	\pm	0.00002				-0.30
	JENDL-3.3	0.98644	\pm	0.00002				-0.53
KENO-VI	ENDF/B-VII.0 (continuous energy)	0.99489	\pm	0.00009				0.32
	ENDF/B-VII.0 (238-group)	0.99461	\pm	0.00008				0.29
	ENDF/B-VI.8 (238-group)	0.99160	\pm	0.00010				-0.01
	ENDF/B-V.2 (238-group)	0.99471	\pm	0.00008				0.30
MONK9(DEV) ^(a)	JEF-2.2	0.9842	\pm	0.0001				-0.75
	JEFF-3.1	0.9854	\pm	0.0001				-0.63
	ENDF/B-VII.0	0.9885	\pm	0.0001				-0.31
	CENDL-3.1	0.9895	\pm	0.0001				-0.21

(a) Results provided by Dave Hanlon from Serco in the United Kingdom.

5.0 REFERENCES

1. J. T. Mihalczo, and D. C. Irving, "Monte Carlo Calculations for Enriched Uranium Metal Assemblies," *Trans. Am. Nucl. Soc.*, # 287 (1964).
2. J. T. Mihalczo, "Multiplication Factor of Uranium Metal by One-Velocity Monte Carlo Calculations," *Nucl. Sci. Eng.*, **27**, 557-563 (1967).
3. J. T. Mihalczo and J. J. Lynn, "Neutron Multiplication Experiments with Enriched Uranium Metal in Slab Geometry," ORNL-CF-61-4-33, Oak Ridge National Laboratory (1961).

HEU-MET-FAST-081

APPENDIX A: TYPICAL INPUT LISTINGS

A.1 MCNP Input Listings

Monte Carlo N-Particle (MCNP) version 5-1.51 calculations were used to calculate results in this evaluation. The Evaluated Neutron Data File library ENDF/B-VII.0 was utilized in the analysis of the experiment and benchmark model biases and uncertainties. The MCNP5 calculations were performed with 1,050 generations that included 1,000,000 neutrons per generation. The k_{eff} estimates did not include the first 50 generations. The statistical uncertainty in k_{eff} is ± 0.00002 (1σ) in all cases.

MCNP Input Listing, Simple Benchmark Model, Table 4.2

```

GROTESQUE by J.D. Bess 7/26/2011
c *****
c                                     HEU-MET-FAST-081
c *****
c Cell Cards
11 11 4.7754E-02 -11:-12:-13          imp:n=1
    *trcl=(0 17.464 0.0) $ Part1
c
21 11 4.7754E-02 -21                  imp:n=1
    *trcl=(12.176 9.343 0.0 52.5 142.5 90 37.5 52.5 90 90 90 0) $ Part2
c
31 11 4.7754E-02 -31                  imp:n=1
    *trcl=(16.333 -1.861 0.0 96.5 186.5 90 6.5 96.5 90 90 90 0) $ Part3
c
41 11 4.7754E-02 -41                  imp:n=1
    *trcl=(9.539 -11.168 0.0 40.5 49.5 90 130.5 40.5 90 90 90 0) $ Part4
c
51 11 4.7754E-02 (-51:-52)           imp:n=1
    *trcl=(0 -17.477 0.0) $ Part5
c
61 11 4.7754E-02 -61                  imp:n=1
    *trcl=(-9.854 -10.944 0.0 42 132 90 48 42 90 90 90 0) $ Part6
c
71 11 4.7754E-02 -71                  imp:n=1
    *trcl=(-16.388 -1.434 0.0 95 5 90 185 95 90 90 90 0) $ Part7
c
81 11 4.7754E-02 -81                  imp:n=1
    *trcl=(-12.029 9.398 0.0 52 38 90 142 52 90 90 90 0) $ Part8
c
91 11 4.7754E-02 (-91:-92:-93)       imp:n=1 $ Part9
c
111 0 -112 #11 #21 #31 #41 #51 #61 #71 #81 #91 imp:n=1 $ TheVoid
112 0 112 imp:n=0

c Surface Cards
c Part1
11 1 rpp -6.3515 6.3515 -6.3515 6.3515 0.000 11.155
12 1 rpp -6.3515 6.3515 -1.2685 3.8115 11.155 13.377
13 1 rpp -6.3515 6.3515 -6.3515 -1.2685 11.155 13.058
c
c Part2
21 2 rcc 0 0 0 0 0 12.918 4.5555
c
c Part3
31 3 rcc 0 0 0 0 0 13.475 5.761
c
c Part4
41 4 rcc 0 0 0 0 0 12.969 4.5525
c
c Part5
51 5 rcc 0 1.7785 8.910 0 0 4.319 4.573
52 5 rpp -3.81 3.81 -6.3515 6.3515 0.000 8.910
c
c Part6
61 6 rcc 0 0 0 0 0 12.974 4.5545
c
c Part7
71 7 rcc 0 0 0 0 0 13.475 5.7495

```

HEU-MET-FAST-081

```

c
c Part8
81 8 rcc 0 0 0 0 0 12.954 4.5565
c
c Part9 (Centerpiece)
91 rpp -6.35 6.35 -6.35 6.35 2.692 8.41
92 rcc 0.593 0.593 0 0 0 2.692 5.757
93 sph 0.268 -0.268 8.41 6.082
c
c Void
112 rcc 0 0 -5 0 0 25 30
c

c Data Cards
kcode 1000000 1 50 1050
ksrc 0 0 0 -0.268 0.268 3.309 -0.593 -0.593 -1.755 12.029 -9.398 0.087
      16.388 1.434 0.140 9.854 10.944 0.134 0 15.698 4.749 0 17.477 0.290
      -9.539 11.168 0.156 -16.333 1.861 0.174 -12.076 -9.343 0.111
      0 17.464 0.150

c
c Transforms
*tr1 0 0 0 0 90 90 90 0 90 90 90 0
*tr2 0 0 0 0 90 90 90 0 90 90 90 0
*tr3 0 0 0 0 90 90 90 0 90 90 90 0
*tr4 0 0 0 0 90 90 90 0 90 90 90 0
*tr5 0 0 0 0 90 90 90 0 90 90 90 0
*tr6 0 0 0 0 90 90 90 0 90 90 90 0
*tr7 0 0 0 0 90 90 90 0 90 90 90 0
*tr8 0 0 0 0 90 90 90 0 90 90 90 0
c
c Material Cards
c HEU
m11 92234.70c 4.7990E-04
      92235.70c 4.4512E-02
      92236.70c 1.8557E-04
      92238.70c 2.5761E-03
c      Total 4.7754E-02

```

MCNP Input Listing, Detailed Benchmark Model, Table 4.1.

```

GROTESQUE by J.D. Bess 7/26/2011
c *****
c                                     HEU-MET-FAST-081
c *****
c Cell Cards
11 11 4.7681E-02 -11:-12:-13          imp:n=1
    *trcl=(0 17.464 0.150) $ Part1
c
21 21 4.8212E-02 -21 22 23          imp:n=1
    *trcl=(12.176 9.343 0.111 52.5 142.5 90 37.5 52.5 90 90 90 0) $ Part2
c
31 31 4.7937E-02 -31 32 33          imp:n=1
    *trcl=(16.333 -1.861 0.174 96.5 186.5 90 6.5 96.5 90 90 90 0) $ Part3
c
41 41 4.7940E-02 -41 42 43          imp:n=1
    *trcl=(9.539 -11.168 0.156 40.5 49.5 90 130.5 40.5 90 90 90 0) $ Part4
c
51 51 4.7769E-02 -52          imp:n=1
    *trcl=(0 -17.477 0.290) $ Part5 - Box
52 52 4.7970E-02 -51 53 54          imp:n=1
    *trcl=(0 -17.477 0.290) $ Part5 - Cylinder
c
61 61 4.7900E-02 -61 62 63          imp:n=1
    *trcl=(-9.854 -10.944 0.134 42 132 90 48 42 90 90 90 0) $ Part6
c
71 71 4.8027E-02 -71 72 73          imp:n=1
    *trcl=(-16.388 -1.434 0.140 95 5 90 185 95 90 90 90 0) $ Part7
c
81 81 4.8017E-02 -81 82 83          imp:n=1
    *trcl=(-12.029 9.398 0.087 52 38 90 142 52 90 90 90 0) $ Part8
c
91 91 4.8092E-02 -92 94 95          imp:n=1 $ Part9 - Cylinder
92 92 4.7758E-02 -91          imp:n=1 $ Part9 - Box

```

HEU-MET-FAST-081

```

93 93 4.8001E-02 -93 91 92          imp:n=1 $ Part9 - Hemisphere
c
111 0 -112 #11 #21 #31 #41 #51 #52 #61 #71 #81 #91 #92 #93 imp:n=1 $ TheVoid
112 0 112 imp:n=0

C Surface Cards
c Part1
11 1 rpp -6.3515 6.3515 -6.3515 6.3515 0.000 11.155
12 1 rpp -6.3515 6.3515 -1.2685 3.8115 11.155 13.377
13 1 rpp -6.3515 6.3515 -6.3515 -1.2685 11.155 13.058
c
c Part2
21 2 rcc 0 0 0 0 0 12.918 4.5555
22 2 rcc 0 4.2735 0 0 0 12.918 0.254
23 2 rcc 0 -4.2735 0 0 0 12.918 0.254
c
c Part3
31 3 rcc 0 0 0 0 0 13.475 5.761
32 3 rcc 0 4.2735 0 0 0 13.475 0.254
33 3 rcc 0 -4.2735 0 0 0 13.475 0.254
c
c Part4
41 4 rcc 0 0 0 0 0 12.969 4.5525
42 4 rcc 0 4.2735 0 0 0 12.969 0.254
43 4 rcc 0 -4.2735 0 0 0 12.969 0.254
c
c Part5
51 5 rcc 0 1.7785 8.910 0 0 4.319 4.573
52 5 rpp -3.81 3.81 -6.3515 6.3515 0.000 8.910
53 5 rcc 0 6.0525 8.910 0 0 4.319 0.254
54 5 rcc 0 -2.4945 8.910 0 0 4.319 0.254
c
c Part6
61 6 rcc 0 0 0 0 0 12.974 4.5545
62 6 rcc 0 4.2735 0 0 0 12.974 0.254
63 6 rcc 0 -4.2735 0 0 0 12.974 0.254
c
c Part7
71 7 rcc 0 0 0 0 0 13.475 5.7495
72 7 rcc 0 4.2735 0 0 0 13.475 0.254
73 7 rcc 0 -4.2735 0 0 0 13.475 0.254
c
c Part8
81 8 rcc 0 0 0 0 0 12.954 4.5565
82 8 rcc 0 4.2735 0 0 0 12.954 0.254
83 8 rcc 0 -4.2735 0 0 0 12.954 0.254
c
c Part9 (Centerpiece)
91 rpp -6.35 6.35 -6.35 6.35 0.937 6.655
92 rcc 0.593 0.593 -1.755 0 0 2.692 5.757
93 sph 0.268 -0.268 6.655 6.082
94 rcc 0.593 4.8665 -1.755 0 0 2.692 0.254
95 rcc 0.593 -3.6805 -1.755 0 0 2.692 0.254
c
c Void
112 rcc 0 0 -5 0 0 25 30
c

c Data Cards
kcode 1000000 1 50 1050
ksrc 0 0 0 -0.268 0.268 3.309 -0.593 -0.593 -1.755 12.029 -9.398 0.087
      16.388 1.434 0.140 9.854 10.944 0.134 0 15.698 4.749 0 17.477 0.290
      -9.539 11.168 0.156 -16.333 1.861 0.174 -12.076 -9.343 0.111
      0 17.464 0.150
c
c Transforms
*tr1 0 0 0 0 90 90 90 1.350 88.65 90 91.35 1.350
*tr2 0 0 0 0 90 90 90 1.4 88.6 90 91.4 1.4
*tr3 0 0 0 0 90 90 90 1.173 88.827 90 91.173 1.173
*tr4 0 0 0 0 90 90 90 1.97 91.97 90 88.03 1.97
*tr5 0 0 0 0 90 90 90 2.58 92.58 90 87.42 2.58
*tr6 0 0 0 0 90 90 90 1.68 91.68 90 88.32 1.68
*tr7 0 0 0 0 90 90 90 1.4 88.6 90 91.4 1.4
*tr8 0 0 0 0 90 90 90 1.1 88.9 90 91.1 1.1
c

```


HEU-MET-FAST-081

```
c Material Cards
c Unit 1
m11      92234.70c 5.1270E-04
          92235.70c 4.4443E-02
          92236.70c 3.2306E-04
          92238.70c 2.4025E-03

c
c Unit 2
m21      92234.70c 4.6998E-04
          92235.70c 4.4940E-02
          92236.70c 1.1530E-04
          92238.70c 2.6867E-03

c
c Unit 3
m31      92234.70c 4.6730E-04
          92235.70c 4.4684E-02
          92236.70c 1.1464E-04
          92238.70c 2.6713E-03

c
c Unit 4
m41      92234.70c 4.6733E-04
          92235.70c 4.4687E-02
          92236.70c 1.1465E-04
          92238.70c 2.6715E-03

c
c Unit 5 - Box
m51      92234.70c 5.1364E-04
          92235.70c 4.4525E-02
          92236.70c 3.2365E-04
          92238.70c 2.4070E-03

c
c Unit 5 - Cylinder
m52      92234.70c 4.6762E-04
          92235.70c 4.4714E-02
          92236.70c 1.1472E-04
          92238.70c 2.6731E-03

c
c Unit 6
m61      92234.70c 4.6694E-04
          92235.70c 4.4650E-02
          92236.70c 1.1455E-04
          92238.70c 2.6693E-03

c
c Unit 7
m71      92234.70c 4.6818E-04
          92235.70c 4.4768E-02
          92236.70c 1.1485E-04
          92238.70c 2.6763E-03

c
c Unit 8
m81      92234.70c 4.6808E-04
          92235.70c 4.4759E-02
          92236.70c 1.1483E-04
          92238.70c 2.6758E-03

c
c Unit 9 - Cylinder
m91      92234.70c 4.6881E-04
          92235.70c 4.4829E-02
          92236.70c 1.1501E-04
          92238.70c 2.6800E-03

c
c Unit 9 - Box
m92      92234.70c 5.1352E-04
          92235.70c 4.4514E-02
          92236.70c 3.2358E-04
          92238.70c 2.4064E-03

c
c Unit 9 - Hemisphere
m93      92234.70c 4.6792E-04
          92235.70c 4.4743E-02
          92236.70c 1.1479E-04
          92238.70c 2.6749E-03

C
```

A.2 KENO-VI Input Listings

KENO-VI calculations (distributed in the SCALE 6.0 software suite) were used to calculate comparison results in this evaluation. The Evaluated Neutron Data File library ENDF/B-VII.0 was utilized in the analysis of the benchmark model bias for removing the tilt of the units and for sample calculations. The KENO-VI calculations were performed with 1,050 generations that included 100,000 neutrons per generation. The k_{eff} estimates did not include the first 50 generations. The statistical uncertainty in k_{eff} is approximately ± 0.00008 (1σ).

KENO Input Listing, Simple Benchmark Model, 4.2

```
'Input generated by GeeWiz SCALE 6.0.13.04 Compiled on January 4, 2010
=csas6
grotesque (simple) by john d. bess at inl
ce_v7_endf
read composition
u-234      1 0 0.0004799 293   end
u-235      1 0 0.044512 293   end
u-236      1 0 0.00018557 293  end
u-238      1 0 0.0025761 293   end
end composition
read parameter
gen=1050
npg=100000
nsk=50
htm=yes
end parameter
read geometry
unit 1
com='unit 1'
cuboid 1   6.3515  -6.3515  -1.2685  -6.3515  13.058  0
cuboid 2   6.3515  -6.3515  3.8115  -1.2685  13.377  0
cuboid 3   6.3515  -6.3515  6.3515   3.8115  11.155  0
cuboid 4   6.3515  -6.3515  6.3515  -6.3515  13.377  0
media 1 1 1
media 1 1 2
media 1 1 3
media 0 1 -1 -2 -3 4
boundary 4
unit 2
com='unit 2'
cylinder 1  4.5555  12.918  0
media 1 1 1
boundary 1
unit 3
com='unit 3'
cylinder 1  5.761  13.475  0
media 1 1 1
boundary 1
unit 4
com='unit 4'
cylinder 1  4.5525  12.969  0
media 1 1 1
boundary 1
unit 5
com='unit 5'
cuboid 1   3.81  -3.81  6.3515  -6.3515  8.91  0
cylinder 2  4.573  13.229  8.91  origin  x=0 y=1.7785 z=0
cuboid 3   4.573  -4.573  6.3515  -6.3515  13.229  0
media 1 1 1
media 1 1 2
media 0 1 -1 -2 3
boundary 3
unit 6
com='unit 6'
cylinder 1  4.5545  12.974  0
media 1 1 1
boundary 1
unit 7
com='unit 7'
cylinder 1  5.7495  13.475  0
media 1 1 1
```

HEU-MET-FAST-081

```

boundary 1
unit 8
com='unit 8'
  cylinder 1 4.5565 12.959 0
  media 1 1 1
boundary 1
unit 9
com='unit 9'
  cylinder 1 5.757 2.692 0 origin x=0.593 y=0.593 z=0
  cuboid 2 6.35 -6.35 6.35 -6.35 8.41 2.692
  sphere 3 6.082 chord +z=0 origin x=0.268 y=-0.268 z=8.41
  cuboid 4 6.35 -6.35 6.35 -6.35 14.492 0
  media 1 1 1
  media 1 1 2
  media 1 1 3
  media 0 1 -1 -2 -3 4
boundary 4
global unit 10
com='grotesque assembly'
  cuboid 1 30 -30 30 -30 15 -5
  hole 1 origin x=0 y=17.464 z=0
  hole 2 origin x=12.176 y=9.343 z=0
  hole 3 origin x=16.333 y=-1.861 z=0
  hole 4 origin x=9.539 y=-11.168 z=0
  hole 5 origin x=0 y=-15.698 z=0
  hole 6 origin x=-9.854 y=-10.944 z=0
  hole 7 origin x=-16.388 y=-1.434 z=0
  hole 8 origin x=-12.029 y=9.398 z=0
  hole 9
  media 0 1 1
boundary 1
end geometry
end data
end

```

KENO Input Listing, Detailed Benchmark Model, Table 4.1

'Input generated by GeeWiz SCALE 6.0.13.04 Compiled on January 4, 2010

=csas6

grotesque (detailed) by john d. bess at inl

ce_v7_endf

read composition

```

u-234      1 0 0.0005127 293  end
u-235      1 0 0.044443 293  end
u-236      1 0 0.00032306 293  end
u-238      1 0 0.0024025 293  end
u-234      2 0 0.00046998 293  end
u-235      2 0 0.04494 293  end
u-236      2 0 0.0001153 293  end
u-238      2 0 0.0026867 293  end
u-234      3 0 0.0004673 293  end
u-235      3 0 0.044684 293  end
u-236      3 0 0.00011464 293  end
u-238      3 0 0.0026713 293  end
u-234      4 0 0.00046733 293  end
u-235      4 0 0.044687 293  end
u-236      4 0 0.00011465 293  end
u-238      4 0 0.0026715 293  end
u-234      5 0 0.00051364 293  end
u-235      5 0 0.044525 293  end
u-236      5 0 0.00032365 293  end
u-238      5 0 0.002407 293  end
u-234      6 0 0.00046762 293  end
u-235      6 0 0.044714 293  end
u-236      6 0 0.00011472 293  end
u-238      6 0 0.0026731 293  end
u-234      7 0 0.00046694 293  end
u-235      7 0 0.04465 293  end
u-236      7 0 0.00011455 293  end
u-238      7 0 0.0026693 293  end
u-234      8 0 0.00046818 293  end
u-235      8 0 0.044768 293  end
u-236      8 0 0.00011485 293  end

```

HEU-MET-FAST-081

```

u-238      8 0 0.0026763 293  end
u-234      9 0 0.00046808 293  end
u-235      9 0 0.044759 293  end
u-236      9 0 0.00011483 293  end
u-238      9 0 0.0026758 293  end
u-234     10 0 0.00046881 293  end
u-235     10 0 0.044829 293  end
u-236     10 0 0.00011501 293  end
u-238     10 0 0.00268 293  end
u-234     11 0 0.00051352 293  end
u-235     11 0 0.044514 293  end
u-236     11 0 0.00032358 293  end
u-238     11 0 0.0024064 293  end
u-234     12 0 0.00046792 293  end
u-235     12 0 0.044743 293  end
u-236     12 0 0.00011479 293  end
u-238     12 0 0.0026749 293  end
end composition
read parameter
  gen=1050
  npg=100000
  nsk=50
  htm=yes
end parameter
read geometry
unit 1
com='unit 1'
  cuboid 1 6.3515 -6.3515 -1.2685 -6.3515 13.058 0
  cuboid 2 6.3515 -6.3515 3.8115 -1.2685 13.377 0
  cuboid 3 6.3515 -6.3515 6.3515 3.8115 11.155 0
  cuboid 4 6.3515 -6.3515 6.3515 -6.3515 13.377 0
  media 1 1 1
  media 1 1 2
  media 1 1 3
  media 0 1 -1 -2 -3 4
  boundary 4
unit 2
com='unit 2'
  cylinder 1 4.5555 12.918 0
  cylinder 2 0.254 12.918 0 origin x=0 y=4.2735 z=0
  cylinder 3 0.254 12.918 0 origin x=0 y=-4.2735 z=0
  media 2 1 1 -2 -3
  media 0 1 2
  media 0 1 3
  boundary 1
unit 3
com='unit 3'
  cylinder 1 5.761 13.475 0
  cylinder 2 0.254 13.475 0 origin x=0 y=4.2735 z=0
  cylinder 3 0.254 13.475 0 origin x=0 y=-4.2735 z=0
  media 3 1 1 -2 -3
  media 0 1 2
  media 0 1 3
  boundary 1
unit 4
com='unit 4'
  cylinder 1 4.5525 12.969 0
  cylinder 2 0.254 12.969 0 origin x=0 y=4.2735 z=0
  cylinder 3 0.254 12.969 0 origin x=0 y=-4.2735 z=0
  media 4 1 1 -2 -3
  media 0 1 2
  media 0 1 3
  boundary 1
unit 5
com='unit 5'
  cuboid 1 3.81 -3.81 6.3515 -6.3515 8.91 0
  cylinder 2 4.573 13.229 8.91 origin x=0 y=1.7785 z=0
  cuboid 3 4.573 -4.573 6.3515 -6.3515 13.229 0
  cylinder 4 0.254 13.229 8.91 origin x=0 y=-2.4955 z=0
  cylinder 5 0.254 13.229 8.91 origin x=0 y=6.0515 z=0
  media 5 1 1
  media 6 1 2 -4 -5
  media 0 1 -1 -2 3
  media 0 1 4
  media 0 1 5

```

HEU-MET-FAST-081

```

boundary 3
unit 6
com='unit 6'
cylinder 1 4.5545 12.974 0
cylinder 2 0.254 12.974 0 origin x=0 y=4.2735 z=0
cylinder 3 0.254 12.974 0 origin x=0 y=-4.2735 z=0
media 7 1 1 -2 -3
media 0 1 2
media 0 1 3
boundary 1
unit 7
com='unit 7'
cylinder 1 5.7495 13.475 0
cylinder 2 0.254 13.475 0 origin x=0 y=4.2735 z=0
cylinder 3 0.254 13.475 0 origin x=0 y=-4.2735 z=0
media 8 1 1 -2 -3
media 0 1 2
media 0 1 3
boundary 1
unit 8
com='unit 8'
cylinder 1 4.5565 12.959 0
cylinder 2 0.254 12.959 0 origin x=0 y=4.2735 z=0
cylinder 3 0.254 12.959 0 origin x=0 y=-4.2735 z=0
media 9 1 1 -2 -3
media 0 1 2
media 0 1 3
boundary 1
unit 9
com='unit 9'
cylinder 1 5.757 2.692 0 origin x=0.593 y=0.593 z=0
cuboid 2 6.35 -6.35 6.35 -6.35 8.41 2.692
sphere 3 6.082 chord +z=0 origin x=0.268 y=-0.268 z=8.41
cuboid 4 6.35 -6.35 6.35 -6.35 14.492 0
cylinder 5 0.254 2.692 0 origin x=0.593 y=4.8665 z=0
cylinder 6 0.254 2.692 0 origin x=0.593 y=-3.6805 z=0
media 10 1 1 -5 -6
media 11 1 2
media 12 1 3
media 0 1 -1 -2 -3 4
media 0 1 5
media 0 1 6
boundary 4
global unit 10
com='grotesque assembly'
cuboid 1 30 -30 30 -30 15 -5
hole 1 origin x=0 y=17.464 z=0.15 rotate a1=0 a2=1.35 a3=0
hole 2 origin x=12.176 y=9.343 z=0.111 rotate a1=-52.5 a2=1.4 a3=0
hole 3 origin x=16.333 y=-1.861 z=0.174 rotate a1=-96.5 a2=1.173 a3=0
hole 4 origin x=9.539 y=-11.168 z=0.156 rotate a1=-139.5 a2=1.97 a3=0
hole 5 origin x=0 y=-15.698 z=0.29 rotate a1=0 a2=-2.58 a3=0
hole 6 origin x=-9.854 y=-10.944 z=0.134 rotate a1=-222 a2=1.68 a3=0
hole 7 origin x=-16.388 y=-1.434 z=0.14 rotate a1=-265 a2=1.4 a3=0
hole 8 origin x=-12.029 y=9.398 z=0.087 rotate a1=-308 a2=1.1 a3=0
hole 9 origin x=0 y=0 z=-1.755
media 0 1 1
boundary 1
end geometry
end data
end

```

A.3 MONK Input Listings

Each MONK9DEV calculation, using either JEF2.2, JEFF3.1, ENDFB/VII.0 or CENDL3.1-based BINGO continuous energy cross section libraries, employed 5000 superhistories per stage, with up to 10 neutron generations tracked per superhistory, and was run for 10 settling stages followed by approximately 70 stages, to achieve a precision of 0.0005. The calculations were repeated twenty five times each to achieve a precision of ± 0.0001 .

MONK Input Listing, Simple Benchmark Model, Table 4.2

* HEU-MET-FAST-081 Grotesque Benchmark

* Simple Model

@loop=1;2;3;4;5;6;7;8;9;10;11;12;13;14;15;16;17;18;19;20;21;22;23;24;25

BEGIN MATERIAL SPECIFICATION
NORMALISE

NUMDEN
MATERIAL Mat_Unit_1
U234 4.7990E-04
U235 4.4512E-02
U236 1.8557E-04
U238 2.5761E-03

MATERIAL Mat_Unit_2 SAME Mat_Unit_1
MATERIAL Mat_Unit_3 SAME Mat_Unit_1
MATERIAL Mat_Unit_4 SAME Mat_Unit_1
MATERIAL Mat_Unit_5 SAME Mat_Unit_1
MATERIAL Mat_Unit_6 SAME Mat_Unit_1
MATERIAL Mat_Unit_7 SAME Mat_Unit_1
MATERIAL Mat_Unit_8 SAME Mat_Unit_1
MATERIAL Mat_Unit_9 SAME Mat_Unit_1

END

BEGIN MATERIAL GEOMETRY
PART Part_Unit_1 CLUSTER
BOX M Mat_Unit_1 -6.3515 -6.3515 0.0 [6.3515*2] [6.3515*2] 11.155
BOX M Mat_Unit_1 -6.3515 -1.2685 11.155 [6.3515*2] [1.2685+3.8115] [13.377-11.155]
BOX M Mat_Unit_1 -6.3515 -6.3515 11.155 [6.3515*2] [6.3515-1.2685] [13.058-11.155]
BOX M 0 -6.3515 -6.3515 0.0 [6.3515*2] [6.3515*2] 13.377

PART Part_Unit_2
ZROD 1 0.0 0.0 0.0 4.5555 12.918
ZONES
M Mat_Unit_2 +1

PART Part_Unit_3
ZROD 1 0.0 0.0 0.0 5.761 13.475
ZONES
M Mat_Unit_3 +1

PART Part_Unit_4
ZROD 1 0.0 0.0 0.0 4.5525 12.969
ZONES
M Mat_Unit_4 +1

PART Part_Unit_5
BOX 1 -4.573 -6.3515 0.0 [4.573*2.0] [6.3515*2] [8.910+4.319]
BOX 2 -3.81 -6.3515 0.0 [3.81*2.0] [6.3515*2] 8.910
ZROD 3 0.0 1.7785 8.910 4.573 4.319
ZONES
M0 +1 -2 -3
M Mat_Unit_5 +2
M Mat_Unit_5 +3

PART Part_Unit_6
ZROD 1 0.0 0.0 0.0 4.5545 12.974
ZONES
M Mat_Unit_6 +1

HEU-MET-FAST-081

```

PART Part_Unit_7
ZROD 1 0.0 0.0 0.0 5.7495 13.475
ZONES
M Mat_Unit_7 +1

PART Part_Unit_8
ZROD 1 0.0 0.0 0.0 4.5565 12.954
ZONES
M Mat_Unit_8 +1

PART Part_Unit_9
BOX 1 -6.35 -6.35 0.0 [6.35*2.0] [6.35*2.0] [8.41+6.082]
ZROD 2 0.593 0.593 0.0 5.757 2.692
BOX 3 -6.35 -6.35 2.692 [6.35*2.0] [6.35*2.0] [8.41-2.692]
ZHEMI 4 0.268 -0.268 8.41 6.082
ZONES
M0 +1 -2 -3 -4
M Mat_Unit_9 +2
M Mat_Unit_9 +3
M Mat_Unit_9 +4

PART Grotesque
ZROD 1 0.0 0.0 -5.0 40.0 25.0
BOX 2 OCEN 0.0 17.464 [13.377/2] [6.3515*2] [6.3515*2] 13.377
ZROD 3 OCEN 12.176 9.343 [(12.918/2)] 4.5555 12.918
ZROD 4 OCEN 16.333 -1.861 [(13.475/2)] 5.761 13.475
ZROD 5 OCEN 9.539 -11.168 [(12.969/2)] 4.5525 12.969
BOX 6 OCEN 0.0 -17.477 [(8.910+4.319)/2] [4.573*2.0] [6.3515*2] [8.910+4.319]
ZROD 7 OCEN -9.854 -10.944 [(12.974/2)] 4.5545 12.974
ZROD 8 OCEN -16.338 -1.434 [(13.475/2)] 5.7495 13.475
ZROD 9 OCEN -12.029 9.398 [(12.954/2)] 4.5565 12.954
BOX 10 OCEN 0.0 0.0 [(8.41+6.082)/2] [6.35*2.0] [6.35*2.0] [8.41+6.082]
ZONES
M 0 +1 -2 -3 -4 -5 -6 -7 -8 -9 -10
P Part_Unit_1 +2
P Part_Unit_2 +3
P Part_Unit_3 +4
P Part_Unit_4 +5
P Part_Unit_5 +6
P Part_Unit_6 +7
P Part_Unit_7 +8
P Part_Unit_8 +9
P Part_Unit_9 +10

END
*****

BEGIN SOURCE GEOMETRY
ZONEMAT
ALL /

END

BEGIN CONTROL DATA
@NUMSET=10 ! Number of Settling Stages
@NUMSTG=1000 ! Maximum Number of Ordinary Stages
@NUMNEUT=5000 ! Number of SuperHistories per Stage
@NGEN=10 ! Number of Generations per SuperHistory
@FACTNU=1.0 ! Estimate of 1/k-eff for 1st stage
@LSTAGE=10 ! Suppress checking of STDV until this ordinary stage
@STDV=0.0005 ! Target Standard Deviation

STAGES [1-@NUMSET] @NUMSTG @NUMNEUT
STDV @STDV
SUPERHIST @NGEN @FACTNU
STDVSTAGE @LSTAGE

DBFON
FISN 7

END

```

HEU-MET-FAST-081

MONK Input Listing, Detailed Benchmark Model, Table 4.1

* HEU-MET-FAST-081 Grotesque Benchmark

* Detailed Model

@loop=1;2;3;4;5;6;7;8;9;10;11;12;13;14;15;16;17;18;19;20;21;22;23;24;25

BEGIN MATERIAL SPECIFICATION
NORMALISE

NUMDEN
MATERIAL Mat_Unit_1
U234 5.1270E-04
U235 4.4443E-02
U236 3.2306E-04
U238 2.4025E-03

MATERIAL Mat_Unit_2
U234 4.6998E-04
U235 4.4940E-02
U236 1.1530E-04
U238 2.6867E-03

MATERIAL Mat_Unit_3
U234 4.6730E-04
U235 4.4684E-02
U236 1.1464E-04
U238 2.6713E-03

MATERIAL Mat_Unit_4
U234 4.6733E-04
U235 4.4687E-02
U236 1.1465E-04
U238 2.6715E-03

MATERIAL Mat_Unit_5_Box
U234 5.1364E-04
U235 4.4525E-02
U236 3.2365E-04
U238 2.4070E-03

MATERIAL Mat_Unit_5_Cyl
U234 4.6762E-04
U235 4.4714E-02
U236 1.1472E-04
U238 2.6731E-03

MATERIAL Mat_Unit_6
U234 4.6694E-04
U235 4.4650E-02
U236 1.1455E-04
U238 2.6693E-03

MATERIAL Mat_Unit_7
U234 4.6818E-04
U235 4.4768E-02
U236 1.1485E-04
U238 2.6763E-03

MATERIAL Mat_Unit_8
U234 4.6808E-04
U235 4.4759E-02
U236 1.1483E-04
U238 2.6758E-03

MATERIAL Mat_Unit_9_cyl
U234 4.6881E-04
U235 4.4829E-02
U236 1.1501E-04
U238 2.6800E-03

MATERIAL Mat_Unit_9_box
U234 5.1352E-04
U235 4.4514E-02

HEU-MET-FAST-081

U236 3.2358E-04
U238 2.4064E-03

MATERIAL Mat_Unit_9_hemi
U234 4.6792E-04
U235 4.4743E-02
U236 1.1479E-04
U238 2.6749E-03

END

BEGIN MATERIAL GEOMETRY
PART Part_Unit_1 CLUSTER
BOX M Mat_Unit_1 0.0 0.0 0.0 12.703 5.083 13.058
BOX M Mat_Unit_1 0.0 5.083 0.0 12.703 5.080 13.377
BOX M Mat_Unit_1 0.0 [5.083+5.080] 0.0 12.703 [12.703-5.083-5.080] 11.155
BOX M 0 0.0 0.0 0.0 12.703 12.703 13.377

PART Part_Unit_2
ZROD 1 0.0 0.0 0.0 [9.111/2] 12.918
ZROD 2 0.0 [-8.547/2] 0.0 [0.508/2] 12.918
ZROD 3 0.0 [8.547/2] 0.0 [0.508/2] 12.918
ZONES
M Mat_Unit_2 +1 -2 -3
M 0 +2
M 0 +3

PART Part_Unit_3
ZROD 1 0.0 0.0 0.0 [11.522/2] 13.475
ZROD 2 0.0 [-8.547/2] 0.0 [0.508/2] 13.475
ZROD 3 0.0 [8.547/2] 0.0 [0.508/2] 13.475
ZONES
M Mat_Unit_3 +1 -2 -3
M 0 +2
M 0 +3

PART Part_Unit_4
ZROD 1 0.0 0.0 0.0 [9.105/2] 12.969
ZROD 2 0.0 [-8.547/2] 0.0 [0.508/2] 12.969
ZROD 3 0.0 [8.547/2] 0.0 [0.508/2] 12.969
ZONES
M Mat_Unit_4 +1 -2 -3
M 0 +2
M 0 +3

PART Part_Unit_5
BOX 1 0.0 0.0 0.0 9.146 12.703 [8.910+4.319]
BOX 2 [(9.146-7.620)/2] 0.0 0.0 7.620 12.703 8.910
ZROD 3 [9.146/2] [12.703-(9.146/2)] 8.910 [9.146/2] 4.319
ZROD 4 [9.146/2] [(12.703-(9.146/2))-(8.547/2)] 8.910 [0.508/2] 4.319
ZROD 5 [9.146/2] [(12.703-(9.146/2))+(8.547/2)] 8.910 [0.508/2] 4.319
ZONES
M0 +1 -2 -3
M Mat_Unit_5_box +2
M Mat_Unit_5_cyl +3 -4 -5
M 0 +4
M 0 +5

PART Part_Unit_6
ZROD 1 0.0 0.0 0.0 [9.109/2] 12.974
ZROD 2 0.0 [-8.547/2] 0.0 [0.508/2] 12.974
ZROD 3 0.0 [8.547/2] 0.0 [0.508/2] 12.974
ZONES
M Mat_Unit_6 +1 -2 -3
M 0 +2
M 0 +3

PART Part_Unit_7
ZROD 1 0.0 0.0 0.0 [11.499/2] 13.475
ZROD 2 0.0 [-8.547/2] 0.0 [0.508/2] 13.475
ZROD 3 0.0 [8.547/2] 0.0 [0.508/2] 13.475
ZONES
M Mat_Unit_7 +1 -2 -3
M 0 +2

HEU-MET-FAST-081

M 0 +3

PART Part_Unit_8

ZROD 1 0.0 0.0 0.0 [9.113/2] 12.954
ZROD 2 0.0 [-8.547/2] 0.0 [0.508/2] 12.954
ZROD 3 0.0 [8.547/2] 0.0 [0.508/2] 12.954

ZONES

M Mat_Unit_8 +1 -2 -3

M 0 +2

M 0 +3

PART Part_Unit_9

BOX 1 0.0 0.0 0.0 12.700 12.700 [2.692+5.718+(12.164/2)]
ZROD 2 [12.700-(11.514/2)] [12.700-(11.514/2)] 0.0 [11.514/2] 2.692
BOX 3 0.0 0.0 2.692 12.700 12.700 5.718
ZHEMI 4 [12.700-(12.164/2)] [12.164/2] [2.692+5.718] [12.164/2]
ZROD 5 [12.700-(11.514/2)] [(12.700-(11.514/2))-(8.547/2)] 0.0 [0.508/2] 2.692
ZROD 6 [12.700-(11.514/2)] [(12.700-(11.514/2))+(8.547/2)] 0.0 [0.508/2] 2.692

ZONES

M0 +1 -2 -3 -4

M Mat_Unit_9_cyl +2 -5 -6

M Mat_Unit_9_box +3

M Mat_Unit_9_hemi +4

M 0 +5

M 0 +6

! Coordinates for Unit 2 from Figure 3.11

@X1_U2=12.176
@X2_U2=12.051
@Y1_U2=9.343
@Y2_U2=9.247
@Z1_U2=0.111
@Z2_U2=[0.111+(12.918/2)]

! Coordinates for Unit 3 from Figure 3.11

@X1_U3=16.333
@X2_U3=16.196
@Y1_U3=-1.861
@Y2_U3=-1.845
@Z1_U3=0.174
@Z2_U3=[0.174+(13.475/2)]

! Coordinates for Unit 4 from Figure 3.11

@X1_U4=9.539
@X2_U4=9.394
@Y1_U4=-11.168
@Y2_U4=-10.999
@Z1_U4=0.156
@Z2_U4=[0.156+(12.969/2)]

! Coordinates for Unit 6 from Figure 3.11

@X1_U6=-9.854
@X2_U6=-9.727
@Y1_U6=-10.944
@Y2_U6=-10.803
@Z1_U6=0.134
@Z2_U6=[0.134+(12.974/2)]

! Coordinates for Unit 7 from Figure 3.11

@X1_U7=-16.388
@X2_U7=-16.224
@Y1_U7=-1.434
@Y2_U7=-1.419
@Z1_U7=0.140
@Z2_U7=[0.140+(13.475/2)]

! Coordinates for Unit 8 from Figure 3.11

@X1_U8=-12.029
@X2_U8=-11.931
@Y1_U8=9.398
@Y2_U8=9.322
@Z1_U8=0.087
@Z2_U8=[0.087+(12.954/2)]

PART Grotesque

HEU-MET-FAST-081

```

ZROD 1 0.0 0.0 -2.0 40.0 40.0
BOX 2 OCEN 0.0 0.0 [-1.755+(2.692+5.718+(12.164/2))/2] 12.700 12.700 [2.692+5.718+(12.164/2)] !
Unit 9
BOX 3 OCEN 0.0 17.464 [0.150+(13.377/2)] 12.703 12.703 13.377 ! Unit 1
XROT -1.350 ABOUT 17.464 0.150
ZROD 4 12.176 9.343 @Z1_U2 [9.111/2] 12.918 ! Unit 2
VZ [@X2_U2-@X1_U2] [@Y2_U2-@Y1_U2] [@Z2_U2-@Z1_U2]
VX [@Y1_U2-@Y2_U2] [@X2_U2-@X1_U2] 0.0
ZROD 5 16.333 -1.861 @Z1_U3 [11.522/2] 13.475 ! Unit 3
VZ [@X2_U3-@X1_U3] [@Y2_U3-@Y1_U3] [@Z2_U3-@Z1_U3]
VX [@Y1_U3-@Y2_U3] [@X2_U3-@X1_U3] 0.0
ZROD 6 9.539 -11.168 @Z1_U4 [9.105/2] 12.969 ! Unit 4
VZ [@X2_U4-@X1_U4] [@Y2_U4-@Y1_U4] [@Z2_U4-@Z1_U4]
VX [@Y1_U4-@Y2_U4] [@X2_U4-@X1_U4] 0.0
BOX 7 OCEN 0.0 -17.477 [0.290+((8.910+4.319)/2)] 9.146 12.703 [8.910+4.319] ! Unit 5
XROT 2.580 ABOUT -17.477 0.290
ZROD 8 -9.854 -10.964 @Z1_U6 [9.109/2] 12.974 ! Unit 6
VZ [@X2_U6-@X1_U6] [@Y2_U6-@Y1_U6] [@Z2_U6-@Z1_U6]
VX [@Y1_U6-@Y2_U6] [@X2_U6-@X1_U6] 0.0
ZROD 9 -16.338 -1.434 @Z1_U7 [11.499/2] 13.475 ! Unit 7
VZ [@X2_U7-@X1_U7] [@Y2_U7-@Y1_U7] [@Z2_U7-@Z1_U7]
VX [@Y1_U7-@Y2_U7] [@X2_U7-@X1_U7] 0.0
ZROD 10 -12.029 9.398 @Z1_U8 [9.113/2] 12.954 ! Unit 8
VZ [@X2_U8-@X1_U8] [@Y2_U8-@Y1_U8] [@Z2_U8-@Z1_U8]
VX [@Y1_U8-@Y2_U8] [@X2_U8-@X1_U8] 0.0
ZONES
M 0 +1 -2 -3 -4 -5 -6 -7 -8 -9 -10
P Part_Unit_9 +2
P Part_Unit_1 +3
P Part_Unit_2 +4
P Part_Unit_3 +5
P Part_Unit_4 +6
P Part_Unit_5 +7
P Part_Unit_6 +8
P Part_Unit_7 +9
P Part_Unit_8 +10

END
*****

BEGIN SOURCE GEOMETRY
ZONEMAT
ALL /

END

BEGIN CONTROL DATA
@NUMSET=10 ! Number of Settling Stages
@NUMSTG=1000 ! Maximum Number of Ordinary Stages
@NUMNEUT=5000 ! Number of SuperHistories per Stage
@NGEN=10 ! Number of Generations per SuperHistory
@FACTNU=1.0 ! Estimate of 1/k-eff for 1st stage
@LSTAGE=10 ! Suppress checking of STDV until this ordinary stage
@STDV=0.0005 ! Target Standard Deviation

STAGES [1-@NUMSET] @NUMSTG @NUMNEUT
STDV @STDV
SUPERHIST @NGEN @FACTNU
STDVSTAGE @LSTAGE

FISN 7

END

```

APPENDIX B: CALCULATED SPECTRAL DATA

The neutron spectral calculations provided below were obtained from the output files for the input decks provided in Appendix A.1 and results in Section 4.1. Only spectral data using the ENDF/B-VII.0 neutron cross section libraries are provided here for the MCNP5 analyses and the ENDF/B-VII.0 (continuous energy) library for the KENO analyses. Cross sections are all continuous energy in the MCNP5 analyses.

B.1 MCNP-Calculated Spectral Data

A summary of the computed neutron spectral data using MCNP5 for the benchmark models is provided in Table B.1.

Table B.1. Neutron Spectral Data for Benchmark Models (MCNP5).

Model	Simple	Detailed
Neutron Cross Section Library	ENDF/B-VII.0	ENDF/B-VII.0
k_{eff}	0.98810	0.99391
$\pm\sigma_k$	0.00002	0.00002
Neutron Leakage (%) ^(a)	55.79	55.51
Fission Fraction, by Energy (%)	Thermal (<0.625 eV)	0.00
	Intermediate	5.06
	Fast (>100 keV)	94.94
Average Number of Neutrons Produced per Fission	2.601	2.601
Energy of Average Neutron Lethargy Causing Fission (MeV)	0.83688	0.83521

(a) The neutron leakage is calculated using the neutron balance tables provided in the MCNP output file. The weight fraction of neutrons lost due to escaping the boundaries of the benchmark model are divided by the total weight fraction of neutron loss.

B.2 KENO-Calculated Spectral Data

A summary of the computed neutron spectral data using KENO-VI for the benchmark models is provided in Table B.2.

Table B.2. Neutron Spectral Data for Benchmark Models (KENO).

Model	Simple	Detailed
Neutron Cross Section Library	ENDF/B-VII.0 (continuous energy)	ENDF/B-VII.0 (continuous energy)
k_{eff}	0.994891	1.001332
$\pm\sigma_k$	0.000091	0.000080
Average Number of Neutrons Produced per Fission	2.60076	2.60045
Energy of Average Neutron Lethargy Causing Fission (MeV)	0.836337	0.834440
Mean Free Path (cm)	1.99267	1.99160